FROM VEERING TRIANGULATIONS TO DYNAMIC PAIRS

SAUL SCHLEIMER AND HENRY SEGERMAN

Abstract. From a transverse veering triangulation (not necessarily finite) we produce a canonically associated dynamic pair of branched surfaces. As a key idea in the proof, we introduce the shearing decomposition of a veering triangulation.

1. Introduction

Mosher, inspired by work of (and with) Christy [14, page 5], and Gabai [14, page 4], introduced the idea of a *dynamic pair of branched surfaces*. These give a combinatorial method for describing and working with pseudo-Anosov flows in three-manifolds. Very briefly, suppose that Φ is such a flow. Then Φ admits a transverse pair of foliations F^Φ and F_Φ, called weak stable and weak unstable, respectively. Carefully splitting both to obtain laminations, and then carefully collapsing, gives a *dynamic pair* of branched surfaces B^Φ and B_Φ. These again intersect transversely, and have other combinatorial properties that allow us to reconstruct Φ (up to orbit equivalence).

Agol, while investigating the combinatorial complexity of mapping tori, introduced the idea of a *veering triangulation* [1, Main construction]. For any pseudo-Anosov monodromy ϕ he provides a canonical periodic splitting sequence of stable train tracks (τ_i^ϕ). This gives a branched surface B^ϕ in the mapping torus $M(\phi)$. Equally well, the splitting sequence of unstable tracks (τ_ϕ^i) gives rise to the branched surface B_ϕ.

More generally, even when not layered [12, Section 4], a veering triangulation $\mathcal{V}$ admits *upper* and *lower branched surfaces* $B^\mathcal{V}$ and $B_\mathcal{V}$, obtained by gluing together standard pieces within each tetrahedron (Section 2.7). Our main result is that these may be isotoped into *split position* and there form a dynamic pair.

Theorem 10.1. *Suppose that $\mathcal{V}$ is a transverse veering triangulation. In split position, the upper and lower branched surfaces $B^\mathcal{V}$ and $B_\mathcal{V}$ form a dynamic pair; this position is canonical. If $\mathcal{V}$ is finite then*

Date: November 6, 2022.

split position is produced algorithmically in polynomial time; also the dynamic train track $B^{\mathcal{V}} \cap B_{\mathcal{V}}$ has at most a quadratic number of edges.

Before giving an outline of the proof of Theorem 10.1, we highlight the main difficulty.

Rem:Difficulty *Remark* 1.1. Suppose that $B^{\mathcal{V}}$ and $B_{\mathcal{V}}$ are in *normal position* within each tetrahedron. This is locally determined, and any other locally determined position can be obtained from normal position by local moves. In normal position, the branched surfaces may coincide on large regions, spanning many tetrahedra; see Section 2.7. Such a region may contain a vertical Möbius band; if so then any small isotopy making $B^{\mathcal{V}}$ and $B_{\mathcal{V}}$ transverse produces "bad" components of $M - (B^{\mathcal{V}} \cup B_{\mathcal{V}})$. We give more details in Section 4.13 and an example in Figure 4.14B. ◇

A more global procedure is thus required. To guide this, we define in Section 5 the *shearing decomposition* associated to $\mathcal{V}$. This is a decomposition of M into solid tori (and possibly solid cylinders in the non-compact case).

Theorem 5.10. *Suppose that $\mathcal{V}$ is a veering triangulation (not necessarily transverse or finite). Then there is an associated shearing decomposition of M canonically associated to $\mathcal{V}$.*

Rem:Section *Remark* 1.2. The shearing decomposition is of independent interest. For example Theorem 5.10 is used by Tsang [20, Corollary 1.2] to show that a transitive pseudo-Anosov flow on a closed three-manifold admits a Birkhoff section with at most two boundary components on orbits of the flow. ◇

With Theorem 5.10 in hand, we give a sequence of coordinatisations inside of the shearing regions. In particular each shearing region is foliated by *horizontal cross-sections*; see Definition 6.3. In Sections 7, 8, and 9 we give a sequence of isotopies to improve the positioning of $B^{\mathcal{V}}$ and $B_{\mathcal{V}}$ relative to each other and relative to the horizontal cross-sections.

Rem:SemiLocal *Remark* 1.3. Our construction is "semi-local" in the following sense. Suppose that $\mathcal{V}$ and $\mathcal{V}'$ are veering triangulations of manifolds M and M'. Suppose that U and U' are isomorphic red components (maximal connected unions of crimped red shearing regions). Then the isomorphism carries the dynamic pair for $\mathcal{V}$ to that of $\mathcal{V}'$ (as intersected with U and U'). ◇

Finally, in Section 10 we verify that $B^{\mathcal{V}}$ and $B_{\mathcal{V}}$, in their final *split position* form a dynamic pair.

Sec:Other

1.4. **Other work.** After Mosher's monograph [14], other appearances of dynamic pairs in the literature include the following. Fenley [9, Section 8] gives an expostion of various examples due to Mosher and proves that leaves of the resulting weak stable and unstable folations have the continuous extension property. Given a uniform one-cochain, Coskunuzer [7, Main Theorem] follows Calegari [4, Theorem 6.2] in producing various laminations, which are collapsed to give a dynamic pair. Calegari [5, Sections 6.5 and 6.6] gives a useful exposition of dynamic pairs and their relation to pseudo-Anosov flows. In particular see his version of examples of Mosher [5, Example 6.49].

Closely related to our overall program is recent work of Agol and Tsang [2, Theorem 5.1]. Starting from a veering triangulation (with appropriate framing), they construct a pseudo-Anosov flow on the filled manifold. They do not use dynamic pairs; instead they apply a different construction of Mosher [14, Proposition 2.6.2]. They identify and remove *infinitesimal cycles*, which are similar in spirit to the vertical Möbius bands mentioned above. Their construction relies on making certain choices, so it is not canonical. Also, it is not clear if the resulting pseudo-Anosov flow recovers the original veering triangulation

1.5. **Future work.** This is the fourth paper in a series of five [17, 18, 10] providing an exact dictionary between veering triangulations (framed with appropriate surgery coefficients) and pseudo-Anosov flows without perfect fits. Theorem 10.1 together with Mosher's work [14, Theorem 3.4.1] gives one direction of the dictionary. In service of our future work, in Appendix A we prove that the "leaf space" of the resulting pseudo-Anosov flow has maximal rectangles corresponding to (via the construction given in [18, Section 5.8]) the original veering tetrahedra.

Acknowledgements. We thank Lee Mosher for enlightening conversations regarding dynamic pairs.

2. Triangulations, train tracks, and branched surfaces

Sec:IdealTriangulations

2.1. **Ideal triangulations.** Suppose that M is a connected three-manifold without boundary. Suppose that $\mathcal{T}$ is a triangulation: a collection of model tetrahedra and a collection of face pairings. (We do not assume here that $\mathcal{T}$ is finite.) We say that $\mathcal{T}$ is an *ideal triangulation* of M if the quotient $|\mathcal{T}|$, minus its zero-skeleton, is homeomorphic to M [19, Section 4.2]. In this case, the degree of each edge of $\mathcal{T}$ is necessarily finite. See Figure 2.2 for an example.

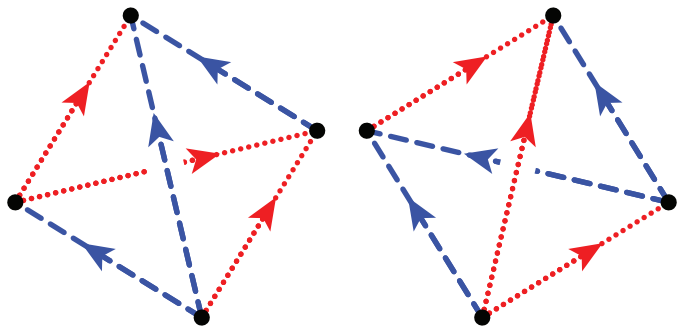

FIGURE 2.2. An ideal triangulation of the complement of the figure-eight knot in the three-sphere. Each edge is equipped with a colour – red (dotted) or blue (dashed) – and an orientation. These determine the face pairings. The flattening (into the plane) makes the triangulation taut and transverse. Note that the taut structure and the orientation determine the veering structure and thus the colours.

Fig:VeerFigEight

A model tetrahedron t is *taut* if every model edge is equipped with a dihedral angle of zero or π, subject to the requirement that the sum of the three dihedral angles at any model vertex is π. It follows that there are exactly two model edges in t with angle π; these do not share any vertex of t. The remaining four model edges, with angle zero, are called *equatorial*. A taut tetrahedron can be flattened into the plane with its equatorial edges forming its boundary; see Figure 2.2. A taut tetrahedron t contains an *equatorial square*: a disk properly embedded in t whose boundary is the four equatorial edges. A ideal triangulation $\mathcal{T}$ of M is a *taut triangulation* if the model tetrahedra are taut and, for every edge e in $|\mathcal{T}|$, the sum of the dihedral angles of the models of e is 2π [12, Definition 1.1].

A taut model tetrahedron t is *transverse* if every model face is equipped with a co-orientation (in or out of t), subject to the requirement that co-orientations agree across model edges of dihedral angle π and disagree across model edges of dihedral angle zero. See Figure 2.3A. A taut triangulation $\mathcal{T}$ of M is a *transverse taut triangulation* if every model tetrahedron is transverse taut and, for every face f in $|\mathcal{T}|$, the associated face pairing preserves the co-orientations of the two model faces [12, Definition 1.2], [13, page 370].

Recall that all model tetrahedra are oriented. A taut model tetrahedron t is *veering* if every model edge is equipped with a colour, red or blue, subject to the following.

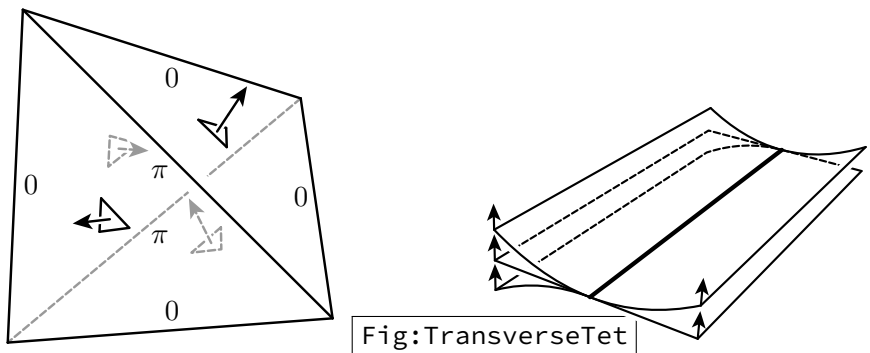

Fig:TransverseTet

(A) Co-orientations and angles in a transverse taut tetrahedron.

Fig:TransverseEdge

(B) Co-orientations around edges can be deduced from the co-orientations on the faces of the model tetrahedra.

Fig:Transverse

FIGURE 2.3

- Viewing any model face (from the outside of the tetrahedron) the non-equatorial edge is followed, in anticlockwise order, by a red equatorial edge.

Suppose that t is a veering tetrahedron. If the two non-equatorial edges of t are both red (blue) then we call t a red (blue) *fan tetrahedron*. If the two non-equatorial edges of t have different colours then we call t a *toggle tetrahedron*. See Figure 2.4A for all four of the possible veering model tetrahedra. Note that the taut structure and the orientation of t determine the colouring of its equatorial edges.

Suppose now that $\mathcal{T}$ is a transverse taut triangulation of M. Then $\mathcal{T}$ is a *transverse veering* triangulation if there is a colouring of the edges of $|\mathcal{T}|$ making all of the model tetrahedra veering [1, Main construction], [12, Definition 1.3]. By the previous paragraph, when such a colouring exists it is unique. Also, if the colouring existsn then the orientations of the model tetrahedra of $\mathcal{T}$ induce an orientation on M. The possible gluings between the various kinds of veering tetrahedra are recorded in Figure 2.4A.

Sec:TrainTracks

2.5. **Train tracks.** For background on train tracks we refer to [15] as well as [19, Chapter 8]. Suppose that $\mathcal{V}$ is a transverse veering triangulation. Suppose that f is a face of $\mathcal{V}$. Let t and t' be the tetrahedra above and below f, respectively. We now define the *upper* and *lower train tracks* τ^f and τ_f in f. The upper track τ^f consists of one switch at each edge midpoint and two branches perpendicular to the edges [1, Figure 11]. The two branches meet only at the switch

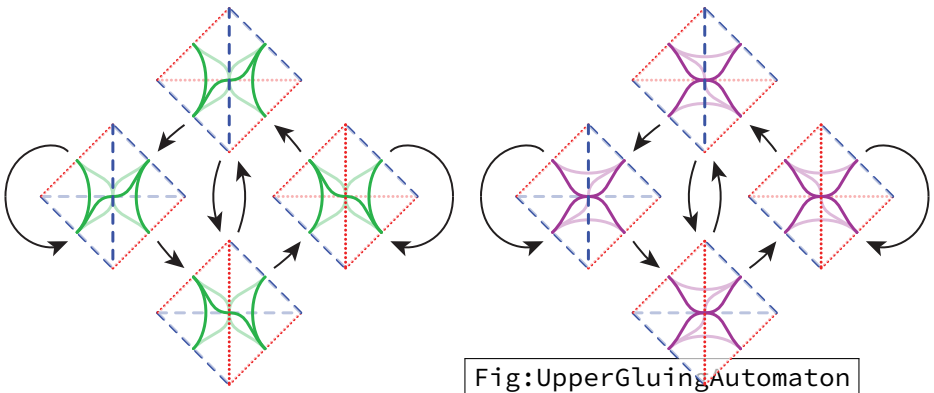

(A) Upper tracks. (B) Lower tracks.

Fig:UpperGluingAutomaton Fig:LowerGluingAutoma

FIGURE 2.4. In both subfigures, above and below we have toggle tetrahedra while left and right we have, respectively, blue and red fan tetrahedra. A black arrow indicates a possible gluing from an upper face of the initial tetrahedron to a lower face of the terminal. Note that fan tetrahedra of different colours never share a face. Finally, inside each tetrahedron t on the left (right) we draw the branched surface B^t (B_t).

Fig:GluingAutomaton

on the non-equatorial edge of t (the tetrahedron *above* f). The lower track τ_f is defined similarly, except the two branches now meet at the switch on the non-equatorial edge of t' (the tetrahedron *below* f). We call the region immediately between the two branches, adjacent to the shared switch, a *track-cusp*. See Figure 2.6. Starting in Section **??** we also discuss slightly more general train tracks in slightly more general surfaces.

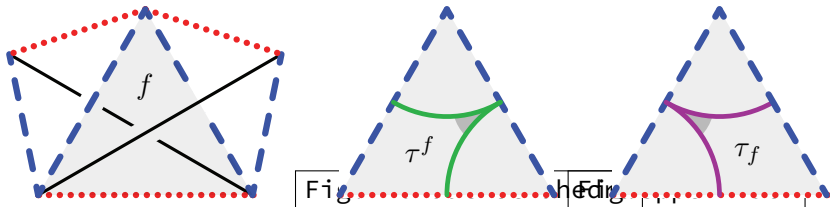

(A) The two taut tetrahedra (above and below) adjacent to a face f. (B) The upper train track τ^f. (C) The lower train track τ_f.

Fig:LowerTrack

FIGURE 2.6

ig:UpperLowerTracks

ec:BranchedSurfaces

2.7. **Branched surfaces.** We refer to [5, Section 6.3] for general background on branched surfaces.

Suppose that M is an oriented three-manifold equipped with a transverse veering triangulation $\mathcal{V}$. Suppose that t is a model tetrahedron of $\mathcal{V}$. The four faces (f_i) of t contain their upper tracks τ^i. These form a graph in ∂t, transverse to the edges of t. This graph bounds a normal quadrilateral and also a pair of normal triangles [6, page 4]. We arrange matters so that the three normal disks meet only along the lower faces of t, so that they are transverse to the equatorial square of t, and so that the union of the normal disks is a branched surface, denoted B^t. We call B^t the *upper branched surface* in t. We define B_t, the *lower branched surface* in t similarly, using the lower tracks τ_i instead of the upper. We finally define $B^{\mathcal{V}} = \cup_t B^t$ and $B_{\mathcal{V}} = \cup_t B_t$ to be the *upper* and *lower branched surfaces* for $\mathcal{V}$ in *normal position*. See Figure 2.9A.

We define the *horizontal branched surface* $B(\mathcal{V})$ to be the union of the faces of $\mathcal{V}$. Here we isotope the faces of $\mathcal{V}$, near their boundaries, to meet the one-skeleton of $\mathcal{V}$ as shown in Figure 2.3B. The horizontal branched surface $B(\mathcal{V})$ is *taut* [13, page 374]; this explains the name *taut ideal triangulations*.

The *branch locus* $\Sigma = \Sigma(B)$ of a branched surface B is the subset of non-manifold points. Each component of $B - \Sigma$ is a *sector* of B. For $B^{\mathcal{V}}$ (and $B_{\mathcal{V}}$) a generic point of its branch locus is locally adjacent to exactly three sectors. The *vertices* of $B^{\mathcal{V}}$ (and $B_{\mathcal{V}}$) are the points of the branch locus locally meeting six sectors. Note that, since we have removed the zero-skeleton from $|\mathcal{V}|$, the horizontal branched surface $B(\mathcal{V})$ has no vertices [13, page 371].

We may move $B^{\mathcal{V}}$ into *dual position* by applying a small upward isotopy of $B^{\mathcal{V}}$. See Figure 2.9B. This done, every tetrahedron t of $\mathcal{V}$ contains exactly one vertex of $B^{\mathcal{V}}$ and every face of $\mathcal{V}$ contains exactly one point of the branch locus. We arrange matters so that the vertex of $B^{\mathcal{V}}$ in t is halfway between the lower edge and the equatorial square of t. Applying a small downward isotopy to $B_{\mathcal{V}}$ produces its dual position. We again arrange matters so that the vertex of $B_{\mathcal{V}}$ in t is halfway between the upper edge (of t) and the equatorial square.

Rem:Dual *Remark* 2.8. In dual position, both $B^{\mathcal{V}}$ and $B_{\mathcal{V}}$ are isotopic to the dual two-skeleton of $\mathcal{V}$. See [10, Remark 6.4]. ◇

We now restate [10, Corollary 6.12].

em:DualMeetsToggles **Lemma 2.10.** *Suppose that M is an oriented three-manifold equipped with a transverse veering triangulation $\mathcal{V}$. In the universal cover, every subray of every branch line of $\widetilde{B}^{\mathcal{V}}$ and of $\widetilde{B}_{\mathcal{V}}$, in dual position, meets toggle tetrahedra.* □

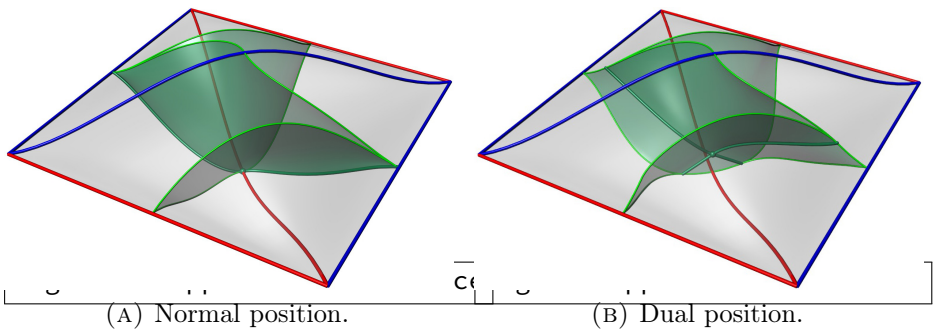

(A) Normal position. (B) Dual position.

pperBranchedSurface

FIGURE 2.9. Two positions of the upper branched surface in a tetrahedron.

Sec:Dynamics

3. DYNAMICS

Suppose that M is a connected oriented three-manifold equipped with a riemannian metric. We follow Mosher [14, page 36] for the next two definitions.

:DynamicVectorField

Definition 3.1. A *dynamic vector field* X on M is simply a non-vanishing vector field. If M has boundary then we require X to be tangent to the boundary of M. ◇

The dynamic vector field X gives us a local notion of *upwards* (the direction of X).

amicBranchedSurface

Definition 3.2. Suppose that M is a three-manifold and X is a dynamic vector field. Suppose that $B^* \subset M$ is a properly embedded branched surface. We say that B^* is a *stable dynamic branched surface* with respect to X if it has the following properties.

- For any point p of any sector of B^*, there is a tangent to the sector, at p, which makes a positive dot product with X. Choosing the largest such gives a vector field X^* on B^*. Integrating X^* gives the *upwards semi-flow*.
- X^* is transverse to the branch locus of B^* and points from the side with fewer sheets to the side with more sheets.
- X^* is never be orthogonal to the branch locus.

The only change needed to define an *unstable dynamic branched surface* B_* is that X_* points from the side with more sheets to the side with fewer. ◇

Remark 3.3. The terms stable and unstable come from the fact that any pseudo-Anosov flow Φ leads to a pair of two-dimensional foliations [5, page 226]. These are the *weak stable* foliation F^Φ and the *weak unstable* foliation F_Φ. If L is a leaf of F^Φ then any two flow lines ℓ and ℓ' in L

are asymptotic in forward time. Finally, the stable branched surface B^Φ carries F^Φ. ◇

Suppose that t is one of the four model transverse veering tetrahedra (shown in Figure 2.4). Let X_t be a non-vanishing vector field in t with the following properties.

- The vector field X_t is orthogonal to each face of t.
- Each orbit of X_t connects a lower face of t with an upper face.
- The branched surfaces B^t and B_t (in dual position) are stable and unstable with respect to X_t.

Now suppose that $\mathcal{V}$ is a transverse taut veering triangulation. We define $X_\mathcal{V}$ by gluing together the vector fields X_t.

Cor:DualDynami

Corollary 3.4. *The upper and lower branched surfaces $B^\mathcal{V}$ and $B_\mathcal{V}$ (in dual position) are, with respect to $X_\mathcal{V}$, stable and unstable dynamic branched surfaces.* □

4. Dynamic pairs

Sec:DynamicPairs

In this section, following Mosher [14, page 52], we give our definition of a *dynamic pair* of branched surfaces. This done, we discuss the main difficulties in proving Theorem 10.1.

4.1. **Complementary components.** Suppose that M is a connected oriented three-manifold equipped with a riemannian metric. Suppose that X is a dynamic vector field on M, as in Definition 3.1. Suppose that B^* and B_* are stable and unstable dynamic surfaces with respect to X. Suppose further that B^* and B_* meet transversely.

:PinchedTetrahedron

Definition 4.2. Suppose that C is a component of $M - (B^* \cup B_*)$. We call C a *pinched tetrahedron* if the closure of C (in the induced path metric on C) is a three-ball, which meets four triangles, with two belonging to $B^* - B_*$ and two belonging to $B_* - B^*$. We call these four triangles the *faces* of C. Each pair of faces meets in a simple arc; altogether these six arcs form the one-skelet one-skeleton of a tetrahedron. The two faces from $B^* - B_*$ meet in a single arc of the branch locus of B^*. Similarly, the two faces from $B_* - B^*$ meet in a single arc of the branch locus of B_*. See Figure 4.3A. ◇

Definition 4.4. We call a foliation of (a three-dimensional region of) M *horizontal* if it is everywhere transverse to X, to B^*, and to B_*. ◇

The birth, life, and death of a pinched tetrahedron play out on the two-dimensional leaves of such a horizontal foliation.

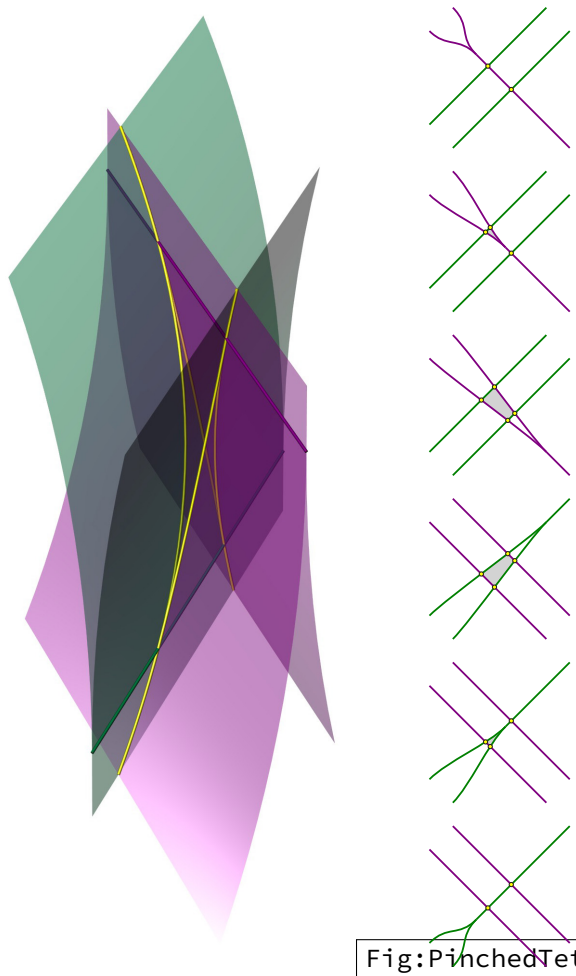

(A) A pinched tetrahedron. (B) Birth, life, and death.

Fig:PinchedTet Fig:LifeAndDeath

FIGURE 4.3. The right shows horizontal slices through the left. See also Figures 2.2, 2.3 and 2.6 of [14].

Fig:PinchedTetBoth

Def:LifeAndDeath

Definition 4.5. Suppose that C is a pinched tetrahedron for B^* and B_*. Since C is simply connected, for the purposes of this definition we may assume that M is simply connected. Suppose that $(H_s)_{s\in\mathbb{R}}$ is a horizontal foliation of a ball in M containing C. As s increases, we move upwards, in the direction of X. Let $\tau^s = H_s \cap B^*$ and $\tau_s = H_s \cap B_*$ be the *upper* and *lower tracks* in H_s respectively. Let $C_s = C \cap H_s$. There are four special times $a < b < c < d$ as follows.

- At time a, the pinched tetrahedron C is born as a track-cusp of τ^a crosses an arc of τ_a, moving forwards.

- For $s \in (a, b)$, the disk C_s is a *green trigon*. It has two sides and a track-cusp in τ^s. The remaining side is in τ_s.
- At time b, the track-cusp of τ^b (on the same branch line) crosses another arc of τ_b, still moving forward.
- For $s \in (b, c)$, the disk C_s is a *quadragon*. Its four sides alternate between τ^s and τ_s.
- At time c, a track-cusp of τ_c crosses an arc of τ^c, moving backwards.
- For $s \in (c, d)$, the disk C_s is a *purple trigon*. It has two sides and a track-cusp in τ_s. The remaining side is in τ^s.
- At time d, the pinched tetrahedron C dies as the track-cusp of τ_d (on the same branch line) crosses an arc of τ^d, still moving backwards. $\diamond$

Figure 4.3B shows $\tau^s \cup \tau_s$ for six representative generic heights.

f:DynamicTorusShell **Definition 4.6.** Suppose that C is a component of $M - (B^* \cup B_*)$. We call C a *dynamic torus shell* if it is homeomorphic to $T^2 \times (0, 1)$. We require that for any ϵ the image of $T^2 \times (0, \epsilon)$ in C is an end of M. The other end of C must have closure (in the path metric) homeomorphic to $T^2 \times (1/2, 1]$. The boundary of this must meet, in alternating fashion, annuli from $B^* - B_*$ and from $B_* - B^*$. The annuli from $B^* - B_*$ are the *stable annuli* of C while the annuli from $B_* - B^*$ are the *unstable annuli* of C. See Figure 4.7.

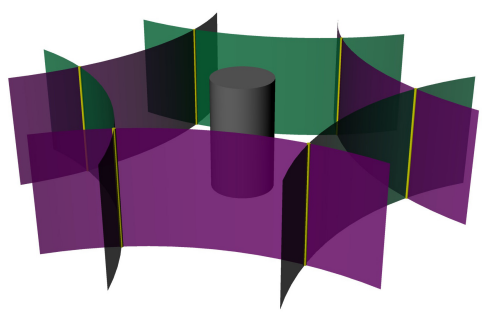

FIGURE 4.7. A section of an annulus or torus shell. The central grey cylinder represents an end of M.

Fig:TorusShell

Taking infinite degree covers of any dynamic torus shell yields (periodic) *dynamic annulus shells* and *dynamic plane shells*. More generally, such shells need not be periodic. This occurs only when neither B^* nor B_* is compact. There are two types of dynamic annulus shell. In one, the frontier is a bi-infinite alternating union of stable and unstable annuli. In the other, the frontier is a finite alternating union of stable

and unstable *strips* of the form $[0,1] \times \mathbb{R}$. There is only one type of dynamic plane shell. Here the frontier is a bi-infinite alternating union of stable and unstable strips. Thus for any dynamic shell C, the components of the frontier (after cutting along $B^* \cap B_*$) are stable and unstable annuli or strips. These annuli or strips are the *faces* of the dynamic shell C. ◇

Definition 4.8. Suppose that C is a complementary region. Suppose that F is an unstable face of C. The components of $F - B_*^{(1)}$ are called the *subfaces* of F. The subfaces of a stable face are defined similarly. ◇

We are now equipped to give our definition of a dynamic pair.

Def:DynamicPair **Definition 4.9.** We say that B^* and B_* form a *dynamic pair* if they satisfy the following.

Itm:Transversality (1) (Transversality): The branched surfaces B^* and B_* intersect transversely.

Itm:Components (2) (Components): Every component of $M - (B^* \cup B_*)$ is either a pinched tetrahedron or a dynamic shell.

Itm:Transience (3) (Transience): For every component F of $B_* - B^*$ there is an unstable face $F' \subset F$ of some dynamic shell so that F' is a sink for the vertical semi-flow restricted to F. The corresponding statement also holds for $B^* - B_*$.

Itm:Separation (4) (Separation): No distinct pair of subfaces of dynamic shells are glued in M. ◇

f:DynamicTrainTrack **Definition 4.10.** Suppose that B^* and B_* form a dynamic pair. Then we define the *dynamic train track* to be the intersection $B^{\mathcal{V}} \cap B_{\mathcal{V}}$. ◇

Rem:ShellsMeet *Remark* 4.11. Dynamic shells (and pinched tetrahedra) may meet each other or themselves along intervals of the dynamic train track. For an example, see Figure 9.12. ◇

Our Definition 4.10 is taken directly from [14, page 54]. Note that our Definition 4.9 is more restrictive than Mosher's [14, page 52]. Mosher allows dynamic shells to meet along subfaces while we do not. He also allows solid torus pieces. We do not require (or allow) solid torus pieces in the cusped case. In the closed case they are necessary; we deal with this as follows.

Remark 4.12. Suppose that γ is a curve in T, a torus boundary component of M. Suppose that C is a torus shell containing T. Suppose that γ meets the dynamic train track (projected from C to T) at least four times. Then Dehn filling M along γ converts C into a solid torus piece $C(\gamma)$. After filling all torus boundary components we arrive at the closed case. ◇

The branched surfaces of a dynamic pair are positioned so as to mimic the relative positions of the stable and unstable foliations of a pseudo-Anosov flow. The transversality of the foliations implies that the branched surfaces should be transverse, and also should not have various kinds of "bigon regions".

Sec:PushOff

4.13. **The naive push-off.** As noted in Remark 1.1, in normal position the branched surfaces $B^{\mathcal{V}}$ and $B_{\mathcal{V}}$ coincide in (at least) all normal quadrilaterals in all fan tetrahedra. To try and fix this, we choose orientations on the edges of $\mathcal{V}^{(1)}$. We then push $B_{\mathcal{V}}$ slightly in the directions of the edge orientations and pull $B^{\mathcal{V}}$ slightly against them. We call this pair of isotopies the *naive push-off*. In Examples 4.15 and 4.16 we see that this sometimes works and sometimes does not. The way in which the naive push-off fails is instructive; as noted in Remark 1.1 the obstructions are non-local.

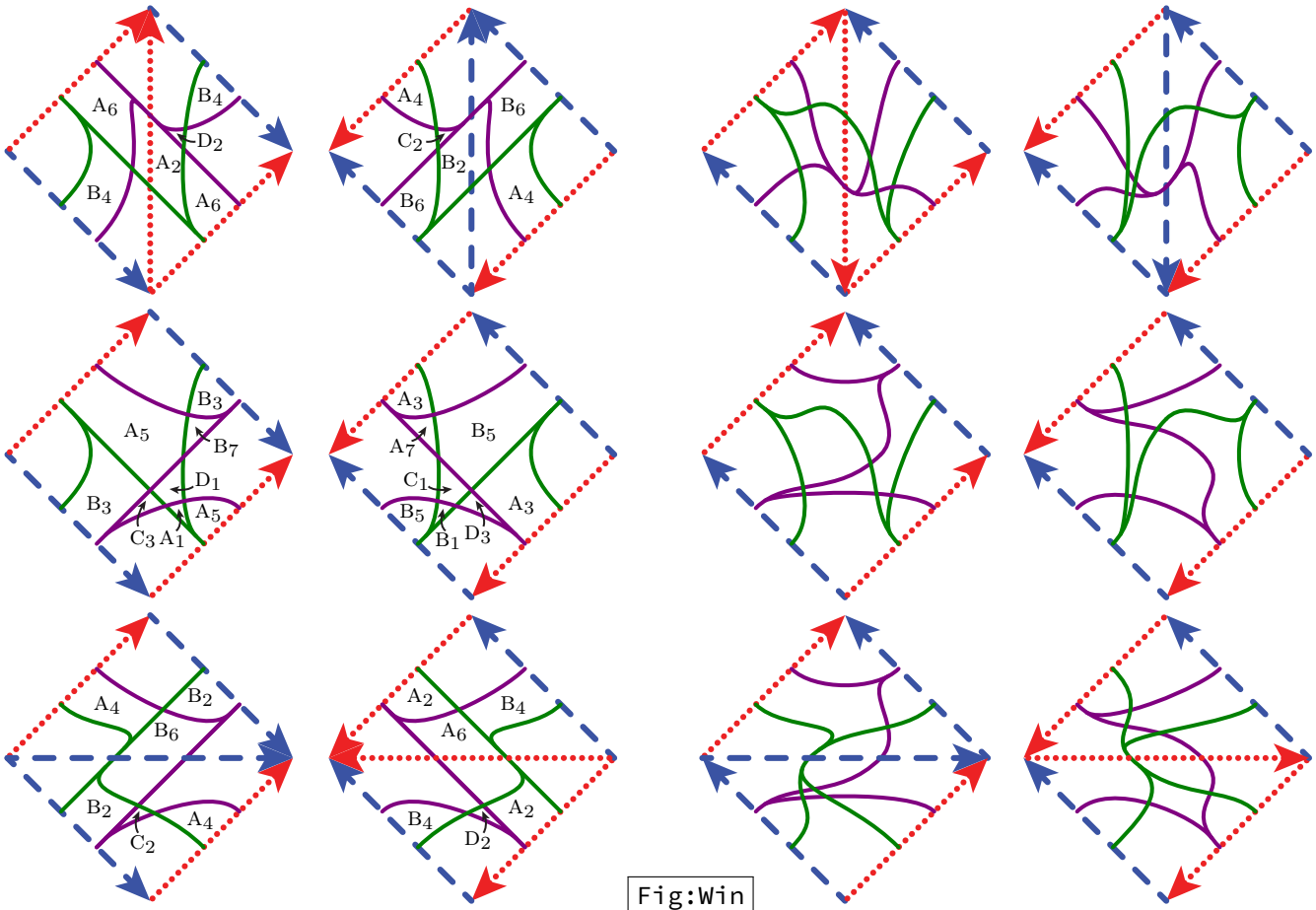

Fig:Win

Fig:Fail

(A) The figure-eight knot complement with the veering triangulation `cPcbbbiht_12`.

(B) The figure-eight knot sibling with the veering triangulation `cPcbbbdxm_10`.

FIGURE 4.14. Canonical triangulations of the figure-eight knot complement and its sibling. Each column shows three slices: the upper and lower faces of, and an equatorial square through, one of the tetrahedra. In the figure-eight knot complement, $B^{\mathcal{V}}$ (green) and $B_{\mathcal{V}}$ (purple) have been naively pushed off each other to produce a dynamic pair. In the sibling, this does not work.

Fig:WinFail

Exa:Wi **Example 4.15.** In Figure 4.14A we draw an exploded view of the veering triangulation on the figure-eight knot complement, as previously introduced in Figure 2.2. The upper and lower train tracks are the result of intersecting $B^{\mathcal{V}}$ and $B_{\mathcal{V}}$ with the faces and equatorial squares of the veering tetrahedra. The naive push-off keeps the dynamic branched surfaces dual to the horizontal branched surface $B = B(\mathcal{V})$ and makes them transverse to each other. Note that no pair of train tracks in any horizontal cross-section form a bigon.

In fact, the push-off makes $B^{\mathcal{V}}$ and $B_{\mathcal{V}}$ into a dynamic pair. Parts (1) and (4) of Definition 4.9 can be checked cross-section by cross-section. For part (2), we have labelled cross-sections through the four pinched tetrahedra A_i through D_i, with subscripts indicating the vertical order. One must check that as we move vertically through the manifold, the sections through the regions assemble to form pinched tetrahedra (see Figure 4.3B) and dynamic torus shells. Note that in Figure 4.14A, as we move downwards from the middle section to the bottom of the two tetrahedra, regions C_1 and D_1 go from being quadragons to being green trigons (and then disappear), but the trigonal stage is not shown. Part (3) must be checked by hand. ◇

Exa:Fai **Example 4.16.** Consider the veering triangulation on the figure-eight knot sibling, shown in Figure 4.14B. Again we push $B_{\mathcal{V}}$ in the direction of the orientations of the edges; this time bigons appear in several of the horizontal cross-sections. In fact there is *no* orientation of the edges that leads to a dynamic pair via the naive push-off. This is because the *mid-surface* for the figure-eight knot sibling is not transversely orientable. For more details see Remark 5.30. ◇

Even if it works, the naive push-off requires making a choice. Thus the resulting dynamic pair is not canonically associated to the initial veering triangulation.

Instead of simply isotoping the branched surfaces horizontally, we will try to "split" them closer to the stable and unstable foliations of the hypothesised pseudo-Anosov flow. To control these splitting isotopies, we must define various decompositions of M (in Sections 5 and 6). We then describe a sequence of isotopies, of each of $B^{\mathcal{V}}$ and $B_{\mathcal{V}}$, through the new decompositions (in Sections 7, 8, and 9).

5. Shearing regions, mid-bands, and the mid-surface

ec:NewCombinatorics

Here we give a decomposition of a veering triangulation into a canonical collection of *shearing regions*. Each of these is either a solid torus or a solid cylinder. We use these to define the *mid-bands* and the *mid-surface*.

earingDecomposition

5.1. **Shearing regions.**

Def:IdealSolid **Definition 5.2.** An *ideal solid torus* U is a solid torus $D^2 \times S^1$, together with a non-empty discrete subset of $(\partial D^2) \times S^1$, called the *ideal points* of U. We define an *ideal solid cylinder* in similar fashion, replacing S^1 by $\mathbb{R}$. ◇

Def:TautSolid **Definition 5.3.** A *taut solid torus (cylinder)* U is a ideal solid torus (cylinder) decorated with a *paring locus* γ containing all of the ideal points of U. The paring locus is a multi-curve $\gamma = \gamma(U)$ meeting every meridional disk exactly twice. There is at least one ideal point on every component of γ. A taut solid torus U has a *mid-band* B; this is either an annulus or a Möbius band, properly embedded in U and disjoint from γ. The mid-band of a taut solid cylinder is instead a strip, $[0,1] \times \mathbb{R}$. In all cases, every boundary compression of the mid-band is required to meet the pairing locus. ◇

Def:TransverseSolid **Definition 5.4.** A *transverse taut solid torus (cylinder)* U is a taut solid torus (cylinder) where $\partial U - \gamma$ has two components, called the *upper* and *lower boundaries* $\partial^+ U$ and $\partial^- U$. These are equipped with transverse orientations that point out of and into U, respectively. Note that all taut solid cylinders can be equipped with such an orientation. ◇

In a transverse taut solid torus the mid-band is necessarily an annulus. In a taut solid cylinder it is necessarily a strip.

Def:ShearingRegion **Definition 5.5.** A *shearing region* U is a taut solid torus or cylinder, together with a *colour* (red or blue) and a squaring of $\partial U - \gamma$, with vertices at the ideal points. All edges contained in the paring locus γ are the opposite colour to U and are called *longitudinal*. All edges not in γ are the same colour as U and are called *helical*. The helical edges form a helix that spirals right or left (as U is red or blue); the helix meets every meridional disk exactly once, transversely. We give the mid-band $B \subset U$ the same colour as U itself. ◇

See Figure 5.6F for the local model of a red shearing region.

earingDecomposition **Definition 5.7.** Suppose that $\mathcal{U}$ is a collection of model shearing regions. Let $\mathcal{U}^{(0)}$ be the union of the ideal points. Suppose furthermore that the shearing regions are glued along all of their squares, respecting the colours of edges and so that every edge has exactly two helical models. We call $\mathcal{U}$ a *shearing decomposition* of $|\mathcal{U} - \mathcal{U}^{(0)}|$. The decomposition is called *transverse* if all of the shearing regions in $\mathcal{U}$ are transverse, and the gluings respect the transverse orientations on the squares. ◇

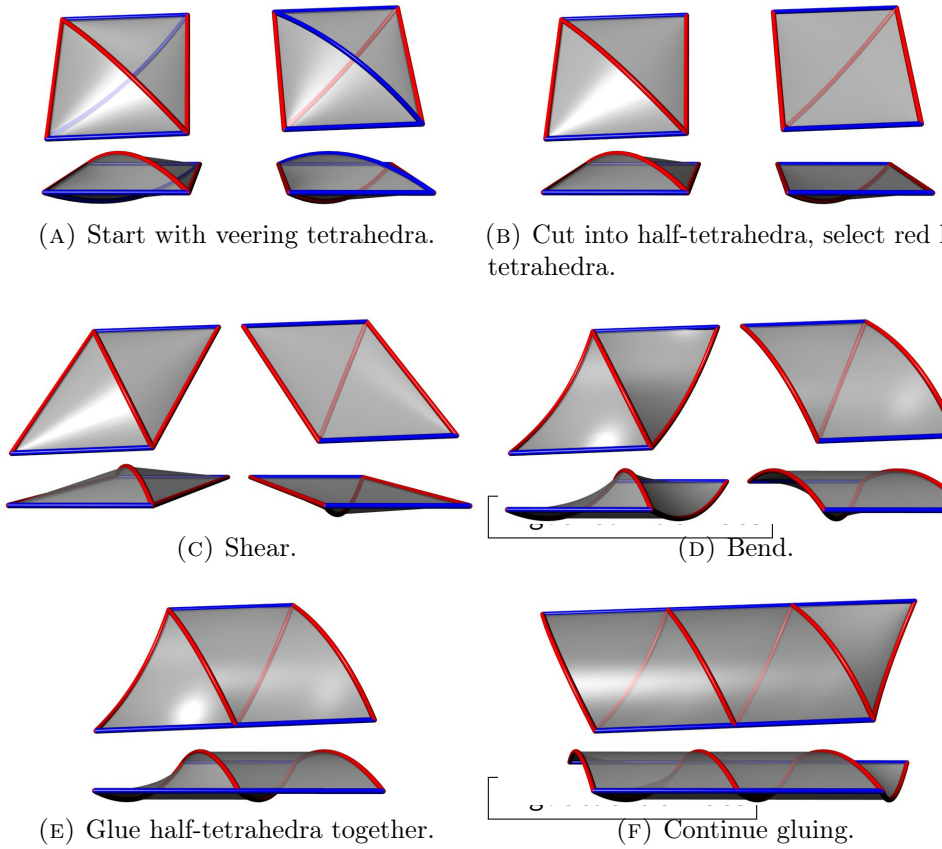

(A) Start with veering tetrahedra.

(B) Cut into half-tetrahedra, select red half-tetrahedra.

Fig:CutVeeringTet

(C) Shear.

(D) Bend.

Fig:PartHalfTets

(E) Glue half-tetrahedra together.

(F) Continue gluing.

Fig:Continuing

idTorusConstruction

FIGURE 5.6. Top and side views of the construction of a red shearing region.

Suppose that $\mathcal{V}$ is a veering triangulation (not necessarily transverse or finite). Recall from Section 2 that there are blue and red fan tetrahedra as well as toggle tetrahedra. Cutting a veering tetrahedron along its equatorial square results in a pair of *half-tetrahedra*; see Figure 5.6B. In every half-tetrahedra there is a unique (up to isotopy) *half-diamond*: this is a triangle, properly embedded in the half-tetrahedron, meeting only the edges of the colour of the π–edge, and those only exactly once at each midpoint. We give a half-diamond the colour of the edges it meets. See Figure 5.8. We arrange matters so that the two half-diamonds in a fan tetrahedron meet along their bases, and so form a full diamond. The two half-diamonds in a toggle t meet in exactly one point: the center of the equatorial square of t. For each half-diamond in a toggle, we colour in black all (but a small neighbourhood of the vertices) of its intersection with the equatorial square. We call this arc the *boundary*

arc of the half-diamond. (In Definition 5.25, the union of the boundary arcs will give the boundary of the *mid-surface*.) Again, see Figure 5.8.

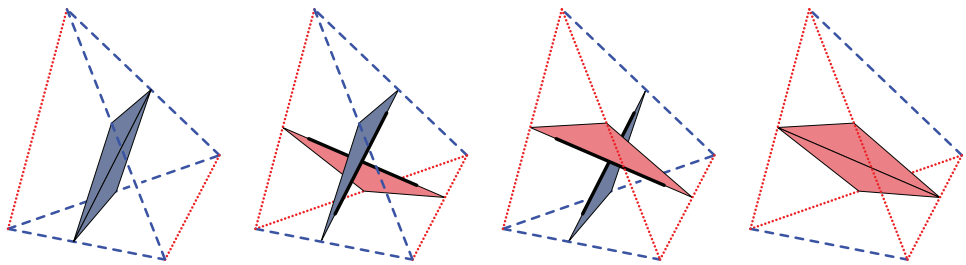

FIGURE 5.8. Diamonds and half-diamonds. Each half-diamond in a toggle has a boundary arc, shown here in black.

Fig:HalfDiamonds

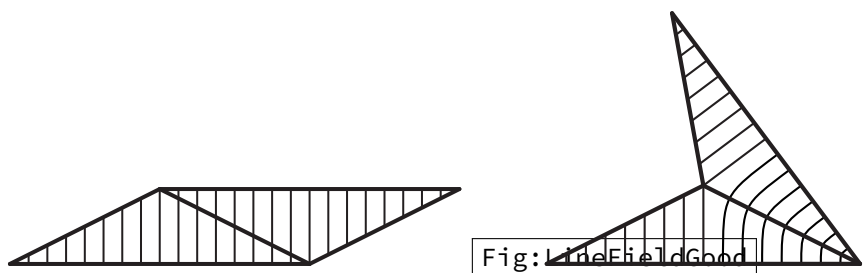

(A) (B)

Fig:LineFieldGood Fig:LineFieldBad

FIGURE 5.9. In Figure 5.9A we see adjacent half-diamonds in a veering triangulation. In Figure 5.9B we see an unpleasant possibility for adjacent half-diamonds in a taut triangulation.

Fig:LineField

earingDecomposition

Theorem 5.10. *Suppose that $\mathcal{V}$ is a veering triangulation (not necessarily transverse or finite). Then there is a shearing decomposition of M canonically associated to $\mathcal{V}$.*

Proof. Suppose that t is a half-tetrahedron and d is its half-diamond. Fix a vertical line field on d as shown in the left-most half-diamond of Figure 5.9A. Let f and f' be the triangular faces of t. The colour of d is the majority colour of the edges of t. Thus the colour of t and d matches the majority colour of both f and f'. Suppose that t is glued to another half-tetrahedron, t', across f'. Let d' be the half-diamond of t'. Thus d' and d have the same colour.

Note that the π-edges of t and t' are distinct edges of the model face f'. (This follows from the definition of a veering triangulation: see Figure 2.6A.) Thus, as shown in Figure 5.9A, we can locally extend the vertical line field on d, through f', to d'. See Figure 5.6E. Let f''

be the other triangular face of t'. Continuing in this fashion in both directions, we obtain a shearing region. The union of the half-diamonds is the mid-band. See Figure 5.11. □

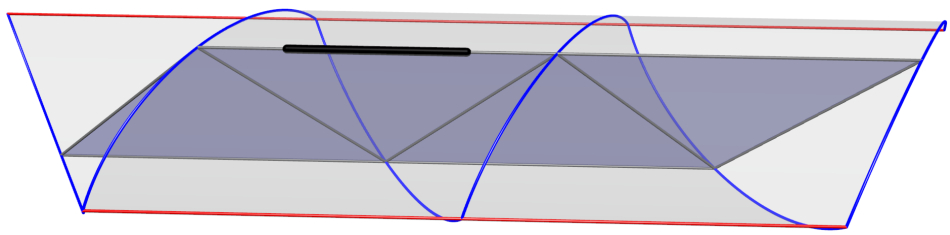

(A) Three-quarters view.

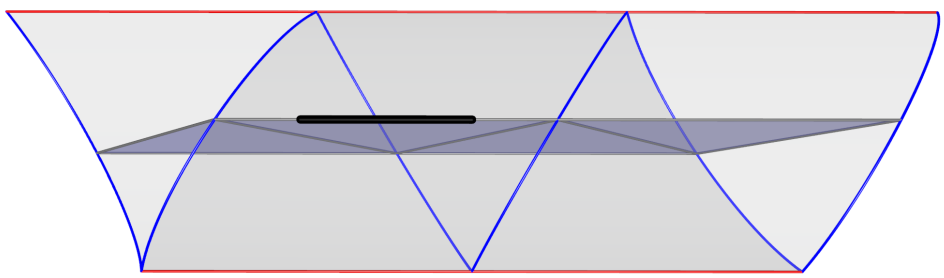

(B) View from above.

FIGURE 5.11. A red shearing region, with embedded mid-band. The boundary arc of the toggle half-diamond is drawn in black.

Fig:SolidTorus

.

We give examples of mid-bands in Figures 5.12 and 5.13. These are taken from the veering census [11].

Rem:Alternate

Remark 5.14. If $\mathcal{V}$ is transverse then the half-tetrahedra in a shearing region alternate between being the upper and lower halves of tetrahedra. That is, the transverse structure on $\mathcal{V}$ induces a transverse structure on the associated shearing decomposition. ◇

Rem:Fractional

Remark 5.15. Suppose that $\mathcal{V}$ is a finite veering triangulation. We may interpret each shearing solid torus as a fractional Dehn twist. A transverse structure on $\mathcal{V}$ equips M with an "upwards" dynamical system. Thus the shearing decomposition (canonically) factors the system as a product of fractional Dehn twists. ◇

Que:CoreCurves

Question 5.16. Let $\gamma(U)$ be a core curve for the shearing region U. Performing certain Dehn fillings along $\gamma(U)$ produces new veering triangulations; see [16] and also [21, Definition 4.1]. Let $\gamma(\mathcal{V})$ be the union of the curves $\gamma(U)$.

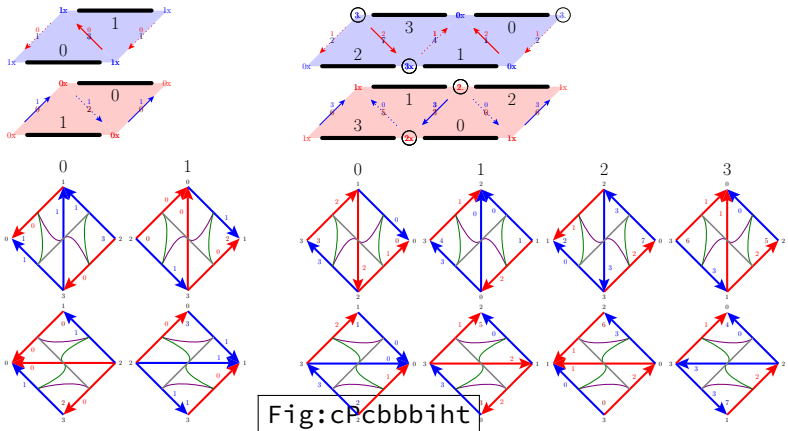

(A) cPcbbbiht_12, m004.

Fig:cPcbbbiht

(B) eLMkbcddddedde_2100, m203.

Fig:eLMkbcddddedde

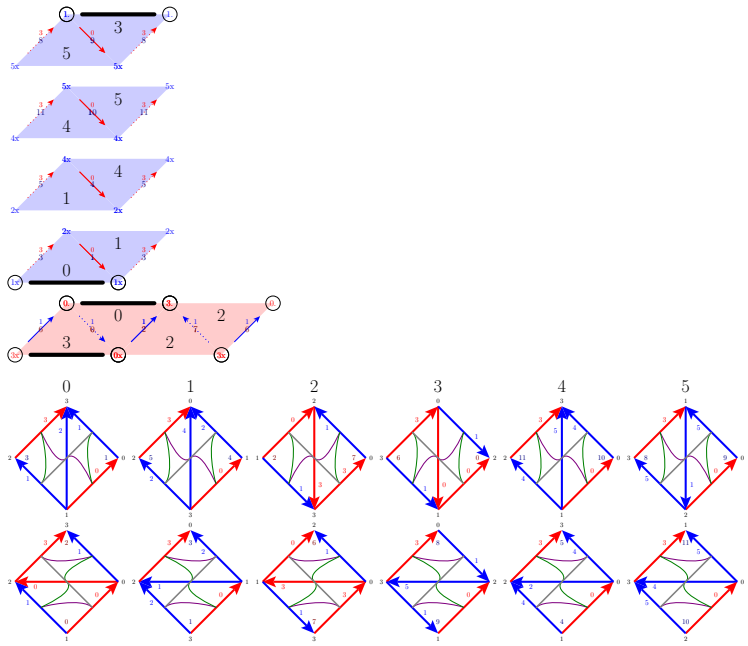

(C) gLLAQbecdfffhhnkqnc_120012, s227.

Fig:gLLAQbecdfffhhnkqnc

FIGURE 5.12. For each example we draw the mid-annuli above and then, in one column per tetrahedron, its upper and lower faces. Drawn on the faces are the intersections with $B^{\mathcal{V}}$ and $B^{\mathcal{V}}$ after the straightening isotopy. See Figures 7.6, 7.7, and 7.8.

ig:ExampleMidAnnuli

Suppose that U and V are a pair of regions. Suppose that the upper boundary of U equals the lower boundary of V. That is, suppose that

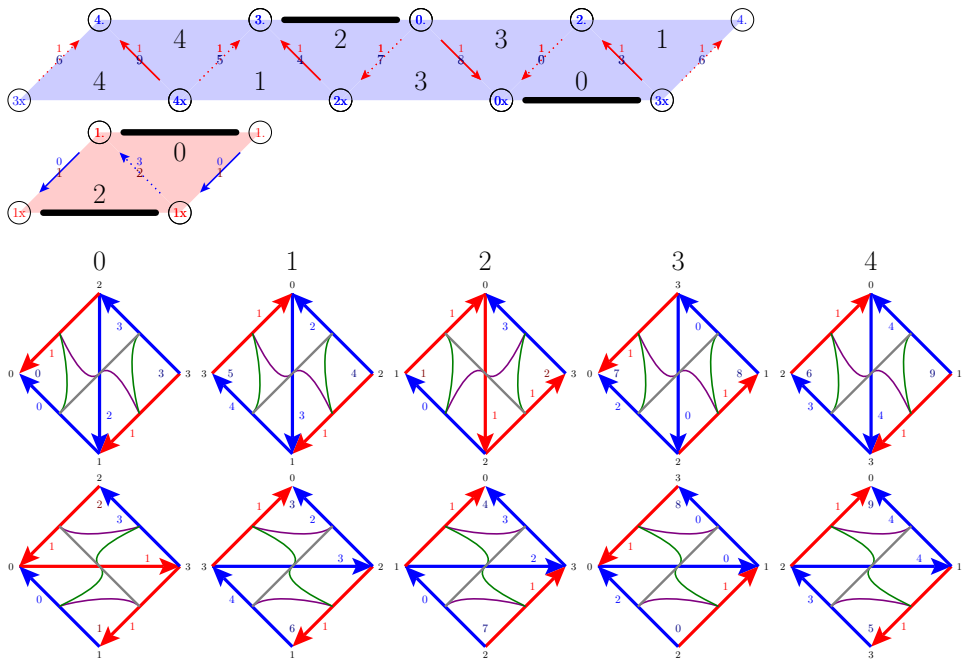

FIGURE 5.13. A veering triangulation for `m115` from the SnapPea census [8]. This is `fLLQccecddehqrwjj_20102` in the census of transverse veering triangulations [11]. As in Figure 5.12, we show the mid-annuli above and the tetrahedron faces below.

g:fLLQccecddehqrwjj

$\partial^+ U = \partial^- V$. Then $\gamma(V)$ is parallel to $\gamma(U)$; accordingly we delete $\gamma(V)$ from $\gamma(\mathcal{V})$.

Now $\gamma(\mathcal{V})$ is a link canonically associated to M and $\mathcal{V}$. What are the geometric properties of $M - \gamma(\mathcal{V})$? $\diamond$

Sec:Crimping

5.17. **Crimping.** Shearing regions give more global coordinates than do individual tetrahedra. Moreover, the interiors of shearing regions are standardised. Here we introduce the *crimped shearing decomposition* of M. This ensures that the union of the shearing regions of a fixed colour is a manifold (with various inward and outward paring loci) containing all of the edges of that colour. One dimension down, crimping improves the way that the red (blue) mid-bands meet. After crimping, their union is the *mid-surface* $\mathcal{S}_R$ ($\mathcal{S}_B$). Crimping is similar to the process of folding, in a train track, all switches with both in- and out-degree bigger than one.

The crimped shearing decomposition is obtained from the shearing decomposition (Theorem 5.10) as follows.

Definition 5.18. Let $E(\mathcal{V})$ be the union of the equatorial squares of all tetrahedra. Thus $E(\mathcal{V})$ is a branched surface. Accordingly we call $E(\mathcal{V})$ the *equatorial* branched surface. $\diamond$

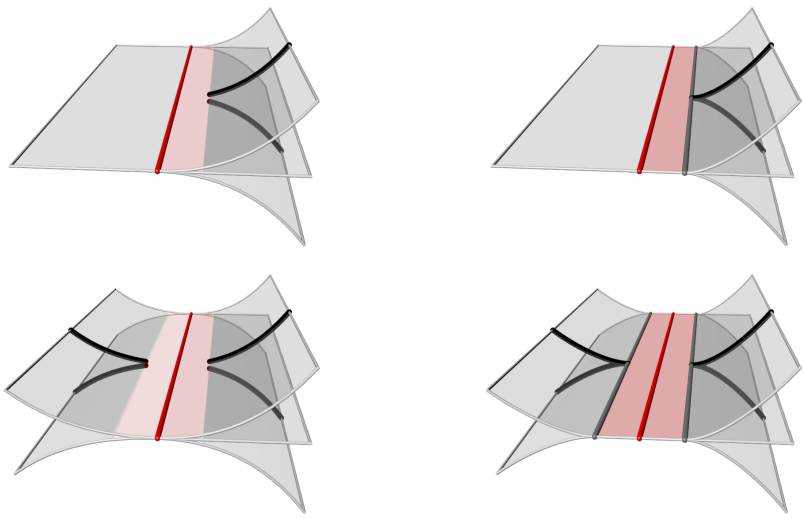

FIGURE 5.19. Top row: an edge $e \in \mathcal{V}^{(1)}$ before and after crimping on the right. No crimping is required on the left. Bottom row: Both sides are crimped. The veering edges are drawn in red, the crimped edges are drawn in grey, and the boundary arcs are drawn in black. The neighbourhoods $N_r(e)$ and $N_\ell(e)$, and the crimped rectangles are shaded red.

Fig:Crimping

Note that an edge $e \in \mathcal{V}^{(1)}$ lies in the branch locus of $E(\mathcal{V})$ if and only if the degree of e (in $E(\mathcal{V})$) is at least three. Suppose that there are at least two squares to the right of e. Let $N_r(e)$ be a collar neighbourhood to the right side of e, taken inside of $E(\mathcal{V})$. (We choose the size of the collar neighbourhood so that it meets the boundary arcs of the relevant half-diamonds each in a single point.) So $N_r(e)$ contains e and a rectangle for every equatorial square to its right. See Figure 5.19 (upper left) for pictures of a possibility for $N_r(e)$. We define $N_\ell(e)$ similarly, again when there are at least two squares to the left of e. Again see Figure 5.19 (lower left). We form the *crimped equatorial* branched surface $E_c(\mathcal{V})$ by *crimping* edges, as follows.

- Fold together all rectangles in $N_r(e)$ to obtain a single rectangle; do the same to the right collar $N_\ell(e)$.

After crimping, as needed, the right and left of every edge, the veering edges of $\mathcal{V}^{(1)}$ are disjoint from the branch locus of $E_c(\mathcal{V})$. Also, there are no vertices in $E_c(\mathcal{V})$. Thus we call the components of $E_c^{(1)}(\mathcal{V})$ *crimped*

edges. Each crimped edge meets an endpoint of each of two boundary arcs. See Figure 5.19 (right) for pictures of possibilities for $E_c(\mathcal{V})$.

Suppose that we had to crimp the right side of e. That is, before crimping, $N_r(e)$ contained two or more rectangles. Then, after crimping, there is a single *crimped rectangle* between e and the crimped edge immediately to the right of e. In our figures we will always colour the crimped edges in grey. Since we draw pictures in the cusped manifold, we will refer to the crimped rectangle as a *crimped bigon*.

Crimping moves the equatorial square of a toggle tetrahedron into $E_c(\mathcal{V})$. There it is subdivided, by the crimped edges, into four crimped bigons and one *toggle square*.

Def:Station **Definition 5.20.** For each corner of each toggle square we take a very small (three-dimensional ball) neighbourhood; this is the *station* associated to that corner. The station is divided into two regions. These are

- an even small smaller neighbourhood of the corner, called the *platform*, and
- the station minus the platform, called the *yard*. ◇

The two boundary arcs (of the mid-surface) in the toggle tetrahedron lie inside of the toggle square. They end at the midpoints of the crimped edges and divide the toggle square into four symmetric regions. See Figure 5.21A. The veering hypothesis implies that a crimped bigon meets, along its crimped edge, exactly two toggle squares: one at the top and one at the bottom of a stack of fan tetrahedra. Similarly, the equatorial square of a fan tetrahedron is subdivided into two crimped bigons and one *fan square*. See Figure 5.21B.

We define the (closures taken in the path metric of) components of $M - E_c(\mathcal{V})$ as *crimped shearing regions*. See Figure 5.22. Let U be a model crimped shearing region. As before, we write ∂^+U and ∂^-U for the upper and lower boundaries of U. Suppose that e and e' bound a crimped bigon B with $e \in \mathcal{V}^{(1)}$ and e' a crimped edge. If B lies in either ∂^+U or ∂^-U then we say that e and e' are *helical* for U. If $B \cap U = e'$ then we say that e and e' are *longitudinal* for U. Note that $\partial^+U \cap \partial^-U$ is the collection of longitudinal crimped edges for U.

As before, we assign U the colour of its helical edges. This colour is opposite to that of each edge of $\mathcal{V}^{(1)}$ that is parallel, across a crimped bigon, to the longitudinal crimped edges of U.

Within U, we replace each triangle of the original triangulation with a corresponding *crimped triangle*. The sides of each crimped triangle consist of two helical edges, one on ∂^+U and one on ∂^-U, and a single longitudinal crimped edge.

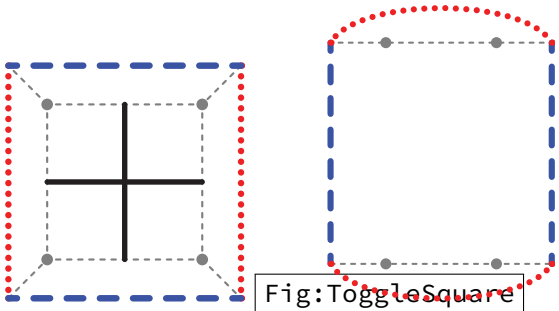

(A) Toggle square. (B) Fan square.

Fig:ToggleSquare Fig:FanSquare

FIGURE 5.21. The toggle square has four adjacent crimped bigons, the fan square has two. Here we draw the boundary arcs (of the half diamonds immediately above and below) on the toggle square in black. The crimped edges are drawn in dashed grey. The corners of the toggle square are contained in their associated stations which are here represented as grey dots.

ig:FanToggleSquares

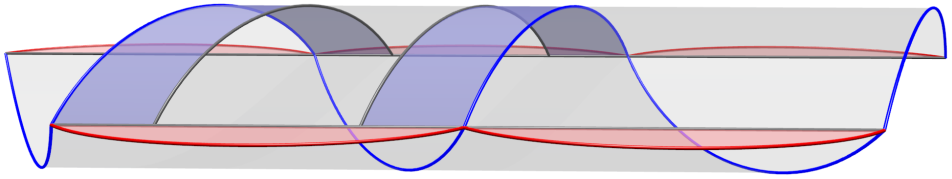

Fig:CrimpedShearingR

(A) View from the side.

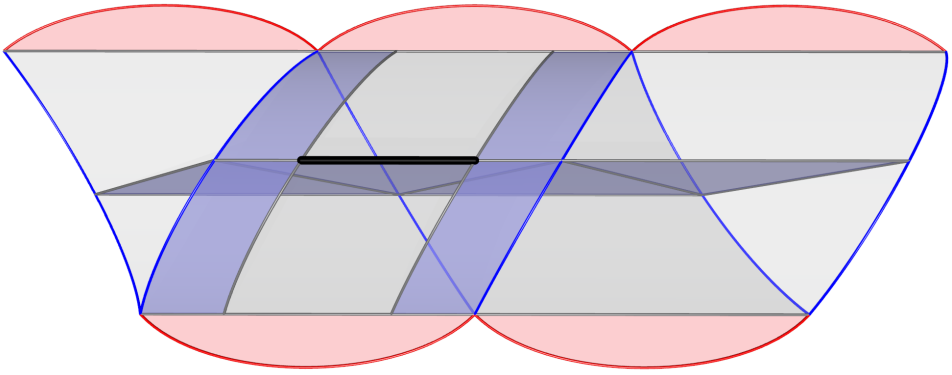

Fig:CrimpedShearingR

(B) View from above, with the mid-band.

FIGURE 5.22. A crimped red solid torus, and incident blue crimped bigons. The crimped edges are drawn in grey and meet the boundary arc in its endpoints.

impedShearingRegion

The union of the crimped shearing regions is again homeomorphic to M; together they form the *crimped shearing decomposition* of M.

Def:Monochromatic **Definition 5.23.** The union of the red crimped shearing regions is the *red part* of the crimped shearing decomposition. A connected component of the red part is a *red component*. We define the *blue part* and *blue components* similarly. ◇

Each red component is a handlebody with inward and outward paring loci. The red part contains all of the red edges of $\mathcal{V}^{(1)}$. Furthermore, its material boundary is the union of the toggle squares. Analogous statements are true for blue components and the blue part.

5.24. **The mid-surface.** The mid-bands sit within the crimped shearing regions in exactly the same way that they sat within the original shearing regions. See Figure 5.22B. We may now glue the mid-bands to each other along their boundaries obtain a surface.

Def:MidSurface **Definition 5.25.** The union of the red mid-bands in the red part gives the *red mid-surface* $\mathcal{S}_R$. We build the blue mid-surface $\mathcal{S}_B$ in a similar fashion. We define the *mid-surface* to be $\mathcal{S} = \mathcal{S}_R \cup \mathcal{S}_B$. ◇

Note that each component of $\mathcal{S}_R$ sits inside, and is a deformation retract of, a red component of the crimped shearing decomposition. In particular, $\mathcal{S}_R$ meets all red edges but no blue edges. A similar statement holds for $\mathcal{S}_B$. Each boundary arc of $\mathcal{S}_R$ meets precisely one boundary arc of $\mathcal{S}_B$; these intersect in a single point at the center of the corresponding toggle square. Lemma 2.10 implies the following.

ComponentBoundaries **Corollary 5.26.** *Every diagonal path in the mid-surface eventually meets a toggle tetrahedron. In particular, every component of $\mathcal{S}_R$ and of $\mathcal{S}_B$ has at least one boundary component.* □

Example 5.27. In Figure 5.13 the red mid-surface has two diagonal paths, both traversing two half-diamonds. The blue mid-surfaces also has two diagonal paths, one traversing six half-diamonds and the other traversing ten. ◇

Every boundary component of the mid-surface runs alternatingly along boundary arcs contained in the upper and lower boundaries of crimped shearing regions. In Figures 5.12 and 5.13 we give several examples; the boundary arcs are indicated by thick black lines. In Figure 5.12A both mid-surfaces are once-holed tori; each boundary component of each mid-surface consists of two boundary arcs. In Figure 5.12B both mid-surfaces are copies of $N_{3,1}$: the non-orientable

surface with one boundary component and three cross-caps. In Figure 5.12C both mid-surfaces are copies of $N_{2,1}$: the once-holed Klein bottle. (This last was the first example of a non-fibered veering triangulation; see [12, Section 4].) Finally, in Figure 5.13 the mid-surfaces are a pair of once-holed Klein bottles, with one having greater area than the other.

Remark 5.28. Mid-surfaces also allow one to see the *walls* of a veering decomposition, as defined by Agol and Tsang [2, Definition 3.3]. For example, in Figure 5.13 there is a wall of width three consisting of the tetrahedra 4 and 1. ◇

Sec:Labelling

5.29. **Labelling the mid-surface.** We now describe the labelling scheme for the mid-surfaces used in the census [11]. This is useful when drawing pictures and discussing examples. Suppose that $\mathcal{V}$ is a finite transverse veering triangulation. We number the tetrahedra, the faces, the edges, and the vertices of the tetrahedra using the conventions from Regina [3]. Regina also provides us with orientations for the edges of $\mathcal{V}^{(1)}$; we will alter these to make them agree, as much as possible, with transverse orientations of mid-annuli.

We give four examples in Figures 5.12 and 5.13. For each example, we draw its mid-annuli and, in one column per tetrahedron, the upper and lower faces for each tetrahedron (viewed from above). On each face we draw the upper (green) and lower (purple) train tracks. (Where these intersect, the intersection is coloured grey.)

In order to draw a mid-band $A = A(U)$ we choose a transverse orientation for it; this then induces a transverse orientation on each half-diamond d of A. In the examples of Figures 5.12 and 5.13 the mid-bands are all annuli and the transverse orientation points into the page.

We label the vertices, edges, and face of the half-diamond d as follows.

- Suppose that v is a vertex of d. We label v with the number of the edge e in $\mathcal{V}^{(1)}$ which contains v. Note that e is helical for U. We append this number with one of the symbols from $\{\cdot, \mathrm{x}\}$. The x means that the orientation of e agrees with the transverse orientation on d; the dot means the opposite. (The x represents the fletching of an arrow, while the dot represents the arrowhead.)
- Suppose that ϵ is a diagonal edge of d. We label ϵ with the number of the face f in $\mathcal{V}^{(2)}$ which contains ϵ; we place the label at the midpoint of ϵ. The vertices of ϵ are already labelled with the numbers of two of the three edges of f. Let e be the third edge of f. Note that e is longitudinal for U. We draw a small

copy of e on top of ϵ and label the copy with the number of e (in the other colour, and using a smaller font). Note that ϵ and e cobound a rectangle in f; we use this rectangle to transport the orientation of e to ϵ. Finally, we draw the arrow dotted or solid as the transverse orientation on d points towards or away from e. (That is, as drawn in Figure 5.12, the edge e is behind or in front of A.)

- Suppose that ϵ is the base of a half-diamond d. If d lies in a toggle then we draw a thick black line on ϵ, to indicate the boundary arc on d.
- Finally, we label d itself with the number of the tetrahedron that contains d.

Suppose that A and B are mid-annuli. Let $\partial^- A$ be the lower boundary of A, *minus* the open boundary arcs. Thus $\partial^- A$ is either a single line, a single circle, or a collection of intervals and at most two rays. We define $\partial^+ B$ similarly. Suppose that A and B are glued to each other, say with a component γ of $\partial^- A$ meeting a component of $\partial^+ B$. (It is also possible for A, say, to be glued to itself.) We call the gluing γ *untwisted* or *twisted* exactly as it does or does not faithfully transport the chosen transverse orientation on A to the one on B.

In Figures 5.12 and 5.13 we indicate a twisted gluing by drawing a small black circle about all vertices of the affected boundary circle or sub-arc. In our examples in Figure 5.12 we have chosen the transverse orientations of the mid-annuli so as to minimize the number of half-twists required.

Rem:Fail *Remark* 5.30. If all gluings are untwisted then the mid-surface is transversely orientable and thus orientable. Conversely, if the mid-surface is orientable then there is a choice of transverse orientations for the mid-bands that ensures that all gluings are untwisted. The naive push-off discussed in Section 4.13 should produce a dynamic pair when and only when the mid-surface is orientable.

Thus, if one is willing to pass to a double cover, then there should be edge orientations making the naive push-off work. However this push-off will not be invariant under the deck transformation. ◇

6. Bigon coordinates

Sec:BigonCoords

In this section we place a coordinate system on the crimped shearing regions (introduced in Section 5.17). We also give a refinement of the crimped shearing decomposition of M and introduce the horizontal cross-sections.

Let B be a *coordinate bigon*: a oriented disk with two marked points x and y in its boundary. The points x and y are the *corners* of B. We equip ∂B with the induced orientation. The two arcs of $\partial B - \{x, y\}$ are denoted by $\partial^+ B$ and $\partial^- B$ respectively. We arrange matters so that $\partial^+ B$ is the arc running from y to x.

We equip B with a pair of transverse foliations: the *horizontal arcs* all meet both corners while the *vertical arcs* all meet $\partial^+ B$ and $\partial^- B$. We orient the former from x to y and the latter from $\partial^- B$ to $\partial^+ B$. See Figure 6.1A.

We subdivide B into a pair of sub-bigons called θ^B (upper) and θ_B (lower). These are shown in Figure 6.1B.

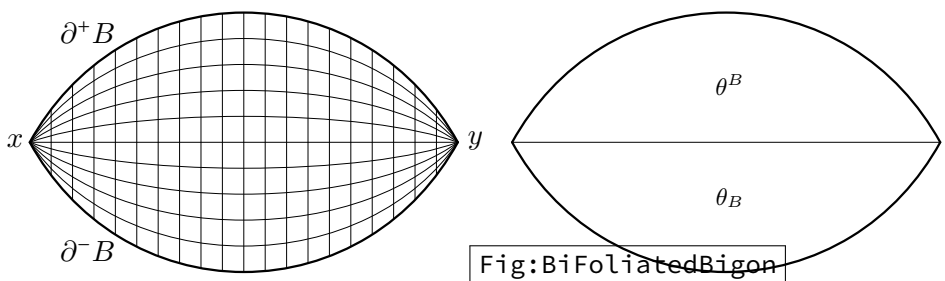

Fig:BiFoliatedBigon Fig:BigonRegions

(A) Model bi-foliated coordinate bigon. (B) Bigon regions.

Fig:Bigon

FIGURE 6.1

Recall that M is oriented and $\mathcal{V}$ is transverse veering. Suppose that U is a model crimped shearing region. Thus U inherits an orientation and, by Remark 5.14, a notion of "upwards". We now choose a homeomorphism h between U and $B \times S^1$ or $B \times \mathbb{R}$, as U is a solid torus or cylinder. We require that h preserve the various orientations. In particular, the upper boundary of B must be sent to the upper boundary of U by h. We call h the *bigon coordinates* for U.

Let Θ^U be the image of $\theta^B \times S^1$ (or $\theta^B \times \mathbb{R}$) in U. We define Θ_U similarly. Note that the upper boundaries of U and Θ^U agree, as do the lower boundaries of U and Θ_U. That is, $\partial^+ U = \partial^+ \Theta^U$ and $\partial^- U = \partial^- \Theta_U$. Also, we have $\partial^- \Theta^U = \partial^+ \Theta_U$. We take $\Theta^{\mathcal{V}} \subset M$ to be the union of the Θ^U, taken over all model crimped shearing regions and then projected to M. We define $\Theta_{\mathcal{V}}$ similarly. The interiors of $\Theta^{\mathcal{V}}$ and $\Theta_{\mathcal{V}}$ are disjoint and their union is M; this is the Θ*–decomposition*.

Rem:NiceBigonCoords *Remark* 6.2. Suppose that U is a blue shearing region. We arrange the metric in U (coming from bigon coordinates) to ensure the following.

(1) In the induced coordinates on $\partial^+ U$ the (pullbacks of the) blue edges of $\mathcal{V}^{(1)}$ are straight and, when viewed from above, have

slope $\sqrt{3}$. Similarly, the blue edges in $\partial^- U$ are straight and, when viewed from above, have slope $-\sqrt{3}$.

Itm:Corners (2) For any toggle square S in $\partial^\pm U$ its corners are very slightly more than one-quarter of the way along the adjacent longitudinal crimped edges.

(3) For $p \in U$ we take $B(p, U)$ to be the coordinate bigon in U containing p. Then the two notions of vertical (coming from the coordinate bigons $B(p, U)$ and the transverse veering structure) agree. Furthermore, the intersection of the mid-band $A(U)$ with any $B(p, U)$ is the central vertical arc of the latter.

See Figure 5.22. We similarly give bigon coordinates to red model crimped shearing regions. ◇

We use the following notations for the various coordinate arcs and surfaces in bigon coordinates.

Def:CrossSection **Definition 6.3.** Suppose that U is a model crimped shearing region. Fix $p \in U$.

- As above, $B(p, U)$ is the coordinate bigon containing p.
- Let $x(p, U) = p \times S^1$ ($p \times \mathbb{R}$) be the horizontal circle (line) in U through p.
- Let $y(p, U)$ be the leaf of the horizontal foliation of $B(p, U)$, through p.
- Let $z(p, U)$ be the leaf of the vertical foliation of $B(p, U)$, through p.
- Let $Y(p, U)$ be the union of the leaves $z(q, U)$ as q ranges over $x(p, U)$. We call $Y(p, U)$ the *vertical band* in U through p.
- Let $Z(p, U)$ be the union of the leaves $x(q, U)$ as q ranges over $y(p, U)$. We call $Z(p, U)$ the *(horizontal) cross-section* in U through p.
- Finally, we define $X(p, U) = B(p, U)$. ◇

Note that the upper and lower boundaries of Θ^U and Θ_U are horizontal cross-sections.

7. Straightening and shrinking

aighteningShrinking

Here we define the *straightening* and *shrinking isotopies*. These are applied to the upper and lower branched surfaces $B^{\mathcal{V}}$ and $B_{\mathcal{V}}$, respectively. These isotopies are local: in each tetrahedron they (and the resulting shrunken position) depend only on the combinatorics of that tetrahedron and its immediate neighbours.

We start in dual position (shown in Figure 2.9B). We *straighten* the branched surfaces to move as many sectors as possible into the

mid-surface $\mathcal{S}$. We *shrink* the branched surfaces to move vertices of $B^{\mathcal{V}}$ down into $\Theta_{\mathcal{V}}$ and those of $B_{\mathcal{V}}$ up into $\Theta^{\mathcal{V}}$.

We now describe in detail the upper straightening and shrinking isotopies of $B^{\mathcal{V}}$. The corresponding lower isotopies of $B_{\mathcal{V}}$ are defined similarly.

Sec:Straightening

7.1. **Straightening.** First, we *straighten*: beginning from dual position (shown in Figure 2.9B) in a fan tetrahedron t, we move the sectors of B^t, meeting the majority colour edges, to coincide with the two half-diamonds of t. In a toggle tetrahedron t, we move the sectors of B^t, meeting the edges of the same colour as the uppermost edge, to contain the upper half-diamond of t.

The resulting position of B^t, in the various crimped half-tetrahedra, is shown in Figures 7.6, 7.7, and 7.8. Each figure has a 180° symmetry about its central vertical axis. We give a global picture of the result in Figure 7.10.

:PictureConventions

Remark 7.2. In our pictures of cross-sections we shade (in grey) all toggle squares. Along a branch interval of $B^{\mathcal{V}}$ within a crimped solid torus, track-cusps are labelled with the same letter. As we move from an upper boundary to a lower the labels, on track-cusps of $B^{\mathcal{V}}$, advance by one letter. Track-cusps of $B_{\mathcal{V}}$ are indicated with small triangles. ◇

Rem:PictureGluing

Remark 7.3. In Figure 7.10 the upper boundary of the blue crimped solid torus U is glued to the lower boundary of U along the fan squares, by a 180° rotation and a (left) shear. As a result, the blue helical veering edges and the red longitudinal veering edges (adjacent to fan squares) match on the top and bottom of U. The red longitudinal veering edges adjacent to the toggle squares do not match. This is because they are glued to the red crimped solid torus V. The upper and lower boundaries of V are also glued, by a 180° rotation and a (right) shear, along the red crimped bigons. ◇

Rem:TangentsShear

Remark 7.4. Suppose that U is a crimped shearing region. Suppose that H and K are $\partial^- U$ and $\partial^+ U$. Let τ^H and τ^K be the intersections of $B^{\mathcal{V}}$ with H and K. So τ^H and τ^K are train tracks. We arrange matters so that τ^H meets longitudinal crimped (helical veering) edges of H with a tangent vector which is parallel to the helical veering (longitudinal crimped) edges of H. We do the same for τ^K. This ensures that tangent vectors match up when sheared by the gluing maps (as in Remark 7.3).

Suppose that H_s parametrises the cross-sections of U, with $H_0 = H$ and $H_1 = K$. As s increases from 0 to 1, the tangent vectors of branches meeting longitudinal crimped edges shear. See Figure 7.10. ◇

Remark 7.5. Observe that all vertices of $B^{\mathcal{V}}$ now lie along the central curve of the middle cross-sections of the crimped shearing regions. (That is, inside of $\partial^- \Theta^{\mathcal{V}} = \partial^+ \Theta_{\mathcal{V}}$.) ◇

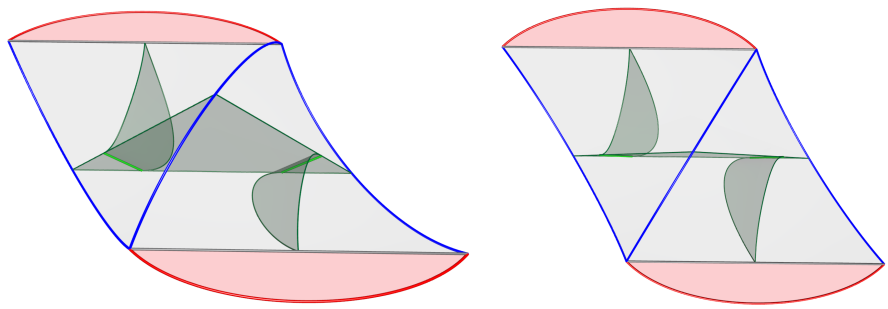

(A) Three-quarter view. (B) Top view.

FIGURE 7.6. Straightened B^t in an upper half-tetrahedron (either toggle or fan).

Fig:UpperHalfTet

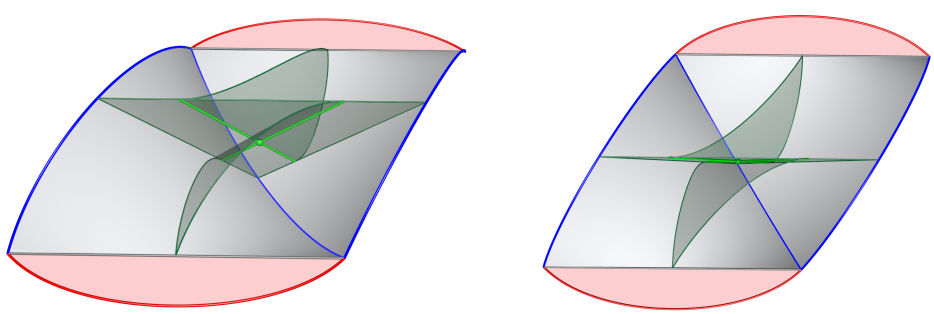

(A) Three-quarter view. (B) Top view.

FIGURE 7.7. Straightened B^t in a lower half-tetrahedron (fan).

Fig:LowerHalfFan

StraightenedDynami

Remark 7.11. As noted in Corollary 3.4 the branched surface $B^{\mathcal{V}}$, when in dual position, is dynamic. Straightening makes parts of $B^{\mathcal{V}}$ vertical. However, the branch locus remains transverse, and not orthogonal, to vertical. Thus the straightened $B^{\mathcal{V}}$ is again dynamic. ◇

Sec:Shrinking

7.12. **Shrinking.** Next we *shrink*: in each crimped shearing region U, we form a very small collar Γ^U of $\partial^+ U$, obtained as a union of horizontal cross-sections $Z(p, U)$. Note that Γ^U is disjoint from the vertices of $B^{\mathcal{V}}$. We now move $B^{\mathcal{V}}$ by a proper isotopy of U which preserves x and y coordinates (in bigon coordinates) and permutes the cross-sections

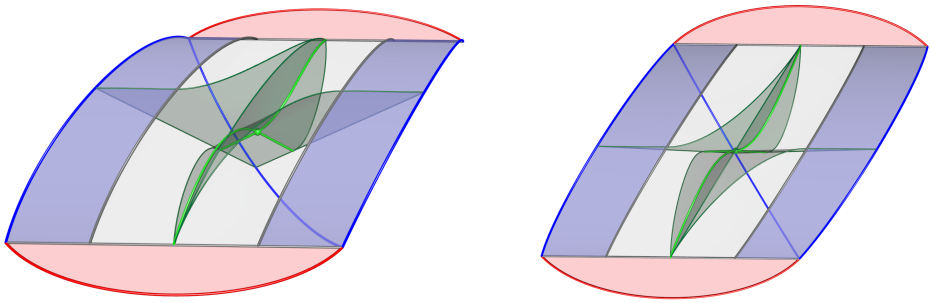

(A) Three-quarter view. (B) Top view.

Fig:LowerHalfToggle

FIGURE 7.8. Straightened B^t in a lower half-tetrahedron (toggle).

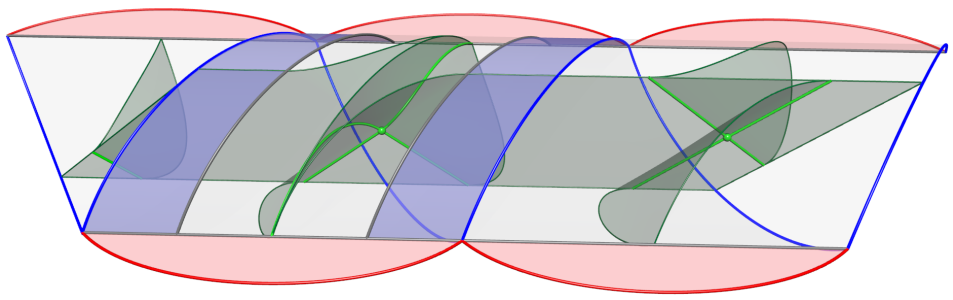

(A) Three-quarter view.

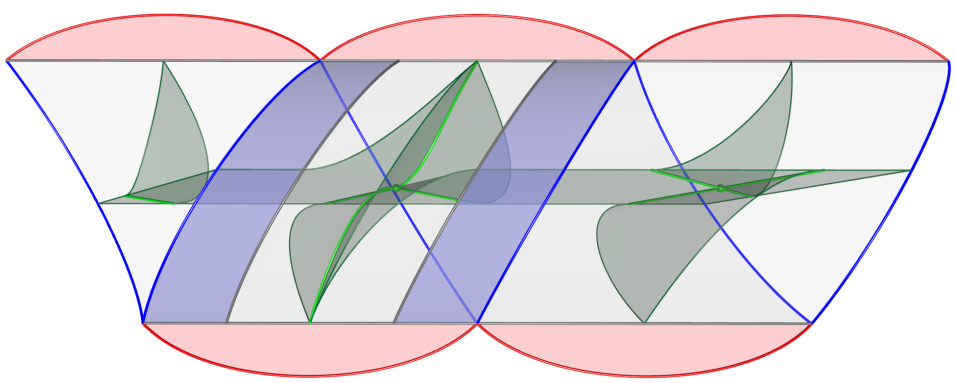

(B) Top view.

impedShearingRegion

FIGURE 7.9. Straightened $B^{\mathcal{V}}$ in a crimped shearing region.

$Z(p, U)$. The isotopy carries the bottom of Γ^U downwards to $\partial^- \Theta^U$ and evenly redistributes the cross-sections below Γ^U inside of Θ_U.

Before the isotopy, $B^{\mathcal{V}}$ was transverse to the equatorial squares. After the isotopy, $B^{\mathcal{V}}$ is almost vertical in all of Θ^U. The intersections of $B^{\mathcal{V}}$

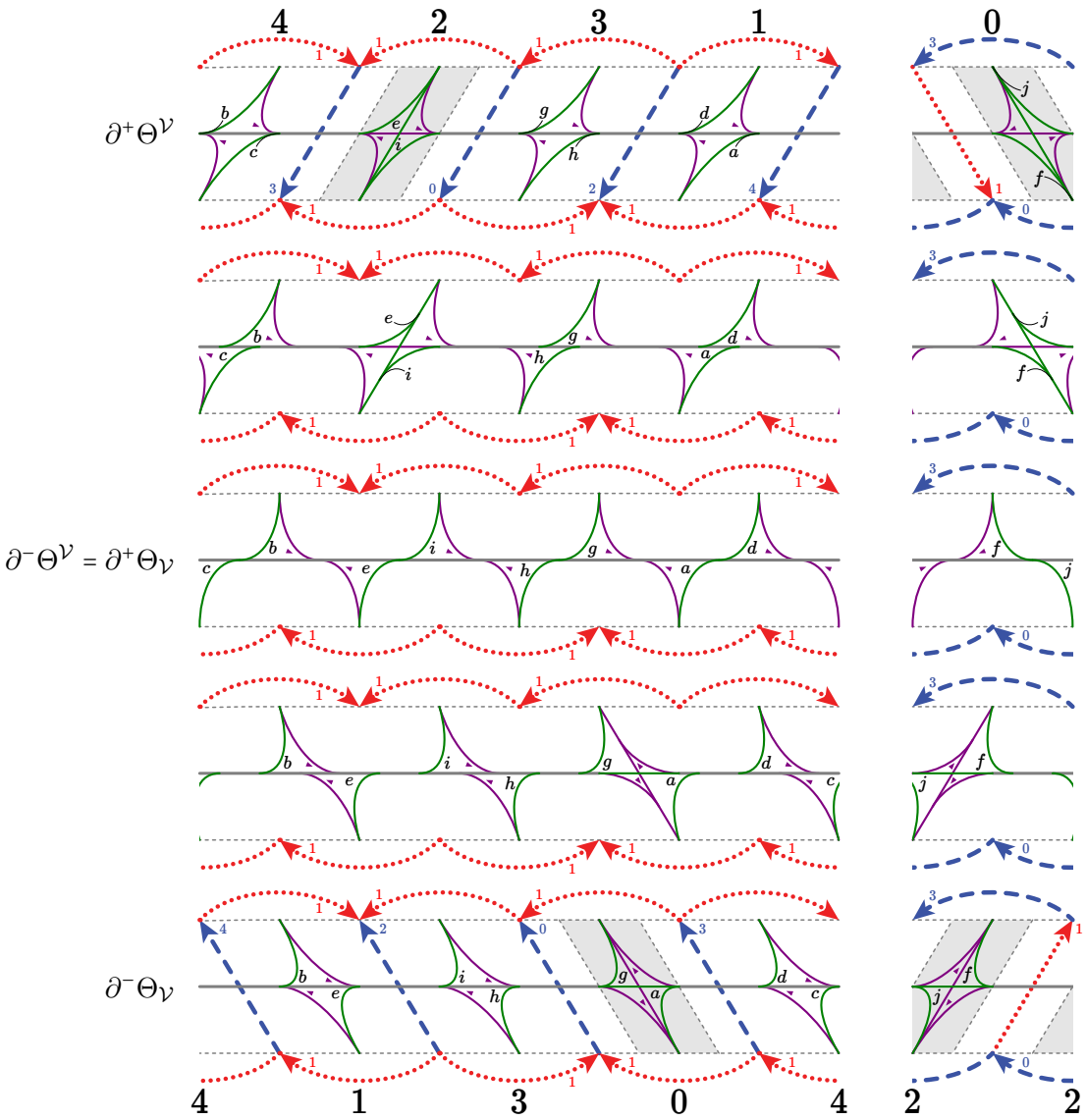

(A) Blue crimped solid torus. (B) Red.

FIGURE 7.10. The intersection of $B^{\mathcal{V}}$ (and $B_{\mathcal{V}}$), after straightening, with various horizontal cross-sections of the crimped shearing decomposition of `fLLQccecddehqrwjj_20102`. Compare with Figure 5.13. We indicate the position of track-cusps with letters or small triangles; sometimes we use a "whisker" pointing from a letter or triangle to the track-cusp itself.

`Fig:m115_straight`

with $\partial^+ U$ and $\partial^- U$ are unchanged by the shrinking isotopy. Note that the shrinking isotopy maintains the 180° symmetry of the branched surfaces B^t. In Figure 7.13 we show the intersection of the shrunken $B^{\mathcal{V}}$ (and $B_{\mathcal{V}}$) with various horizontal cross-sections.

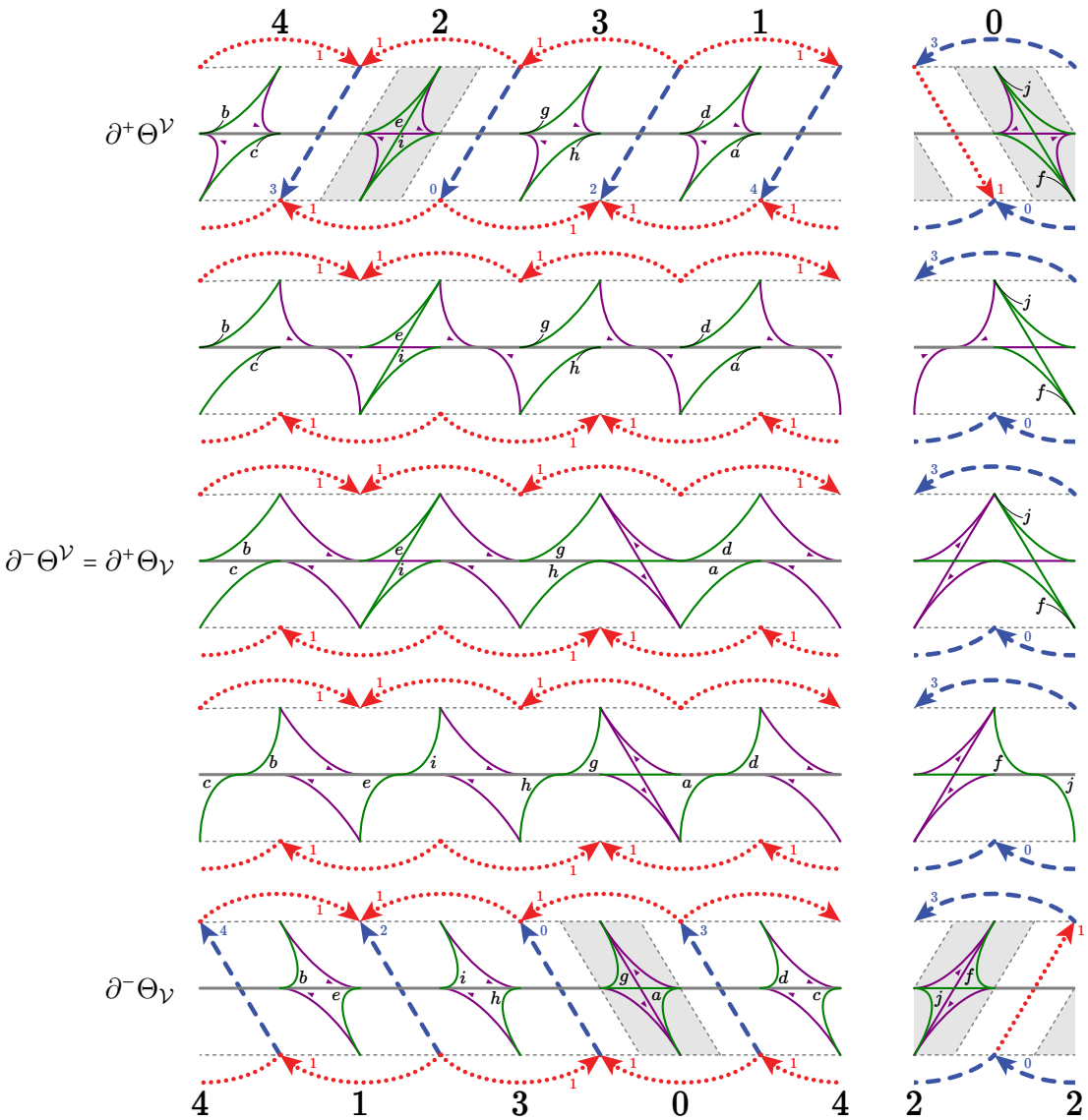

(A) Blue crimped solid torus. (B) Red.

FIGURE 7.13. The intersection of $B^{\mathcal{V}}$ (and $B_{\mathcal{V}}$), after shrinking, with various horizontal cross-sections of the crimped shearing decomposition of `fLLQccecddehqrwjj_20102`. Compare with Figure 7.10.

Fig:m115_shrink

runkenTangentsShea

Remark 7.14. Note that the shearing of tangent vectors, as in Remark 7.4, now occurs in $\Theta_{\mathcal{V}}$ for $B^{\mathcal{V}}$ (and in $\Theta^{\mathcal{V}}$ for $B_{\mathcal{V}}$). ◇

Rem:ShrunkenDynami

Remark 7.15. Shrinking permutes cross-sections; thus by Remark 7.11 the shrunken branched surface $B^{\mathcal{V}}$ is again dynamic. ◇

Sec:Parting

8. Parting

Here we define the *parting isotopies*. These are applied to the upper and lower branched surfaces $B^{\mathcal{V}}$ and $B_{\mathcal{V}}$, respectively. These isotopies are again local: in each tetrahedron they (and the resulting parted position) depend only on the combinatorics of that tetrahedron and its immediate neighbours.

We now concentrate on $B^{\mathcal{V}}$. We start in shrunken position (shown in Figure 7.13). In each cross-section of $\Theta^{\mathcal{V}}$, and near each crimped edge, we will move $B^{\mathcal{V}}$ towards the correct station (corner) of the relevant toggle square. We also will isotope branches of $B^{\mathcal{V}}$ in cross-sections of $\Theta^{\mathcal{V}}$ to be (almost) line segments (in bigon coordinates). As in shrunken position, the parted position of $B^{\mathcal{V}}$ in $\Theta^{\mathcal{V}}$ will almost be a product.

This done, we will move $B^{\mathcal{V}}$ carefully downward in $\Theta_{\mathcal{V}}$. This makes the intersection of $B^{\mathcal{V}}$ with the cross-sections into a sequence of train tracks as follows. As they move up through $\Theta_{\mathcal{V}}$ they first perform a *neighbourhood splitting* where track-cusps move along their *parting routes*. They next perform a *graphical isotopy* where the track-cusps are (almost) motionless and the branches straighten to become (almost) line segments.

The branched surface $B_{\mathcal{V}}$ moves in a similar way, but swapping $\Theta^{\mathcal{V}}$ and $\Theta_{\mathcal{V}}$. The ideas of neighbourhood splitting and graphical isotopy will be used once (in sapce) in this section and three times (in time and in space) in Section 9. We use them to fill in the isotopy from parted position to the final position.

Sec:PartingUp

8.3. Parting in $\Theta^{\mathcal{V}}$.

We now describe the *parting isotopy* in $\Theta^{\mathcal{V}}$.

Suppose that U is a crimped blue shearing region. Suppose that e' is a crimped longitudinal edge for U. Suppose that e is the associated red veering edge and let C be the crimped bigon which e and e' cobound. Suppose that $S \subset \partial^+ U$ is the upper toggle square meeting e'. We equip C with the anti-clockwise orientation, as viewed from above. This induces orientations on e and e'. Let $c = C \cap B^{\mathcal{V}}$. The parting isotopy in Θ^U fixes $c \cap e$ and moves $c \cap e'$ along e', against the orientation of e' (given just above), until it arrives at the platform of the station at the corner of the toggle square S. (If, instead, U is red, then we move $c \cap e'$ along e', following the orientation of e', again until it arrives at

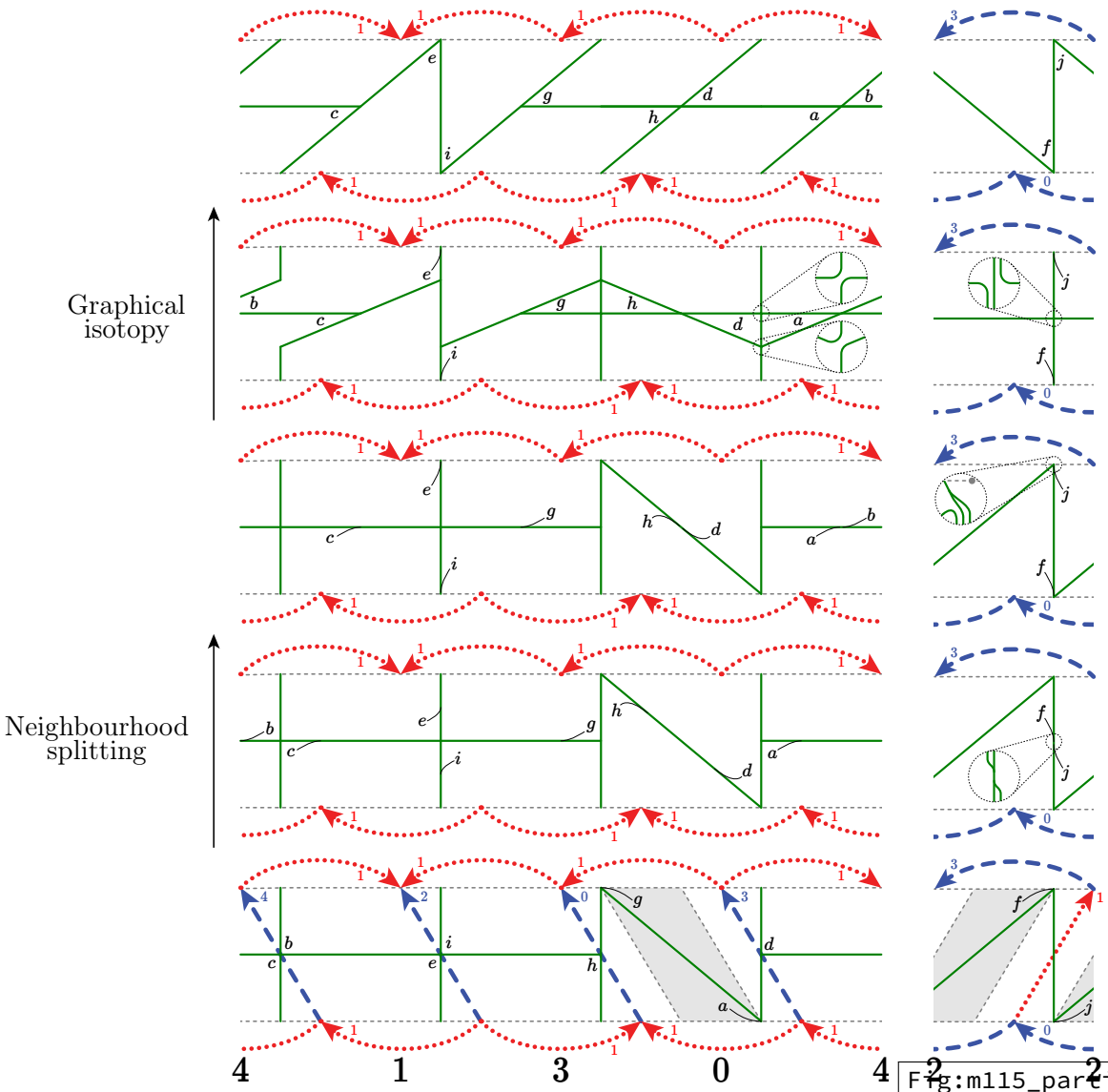

(A) Blue crimped solid torus. (B) Red.

Fig:m115_parting_in_theta_U_blue

FIGURE 8.1. The result B_1 of the parting isotopy in $\Theta_{\mathcal{V}}$ where $\mathcal{V}$ is `fLLQccecddehqrwjj_20102`. The five diagrams show (from the bottom moving up) $B_1 \cap C_s$ for $s \in (0, 1/4, 1/2, 3/4, 1)$. The bottom cross-section contains blue helical edges.

_parting_in_theta_U

the platform of its station.) To see this motion, compare top lines of Figures 7.13 and 8.2.

In $\partial^+ U$ we also move track-cusps outwards in fan squares until they arrive close to the midpoint of a helical edge. In lower cross-sections of

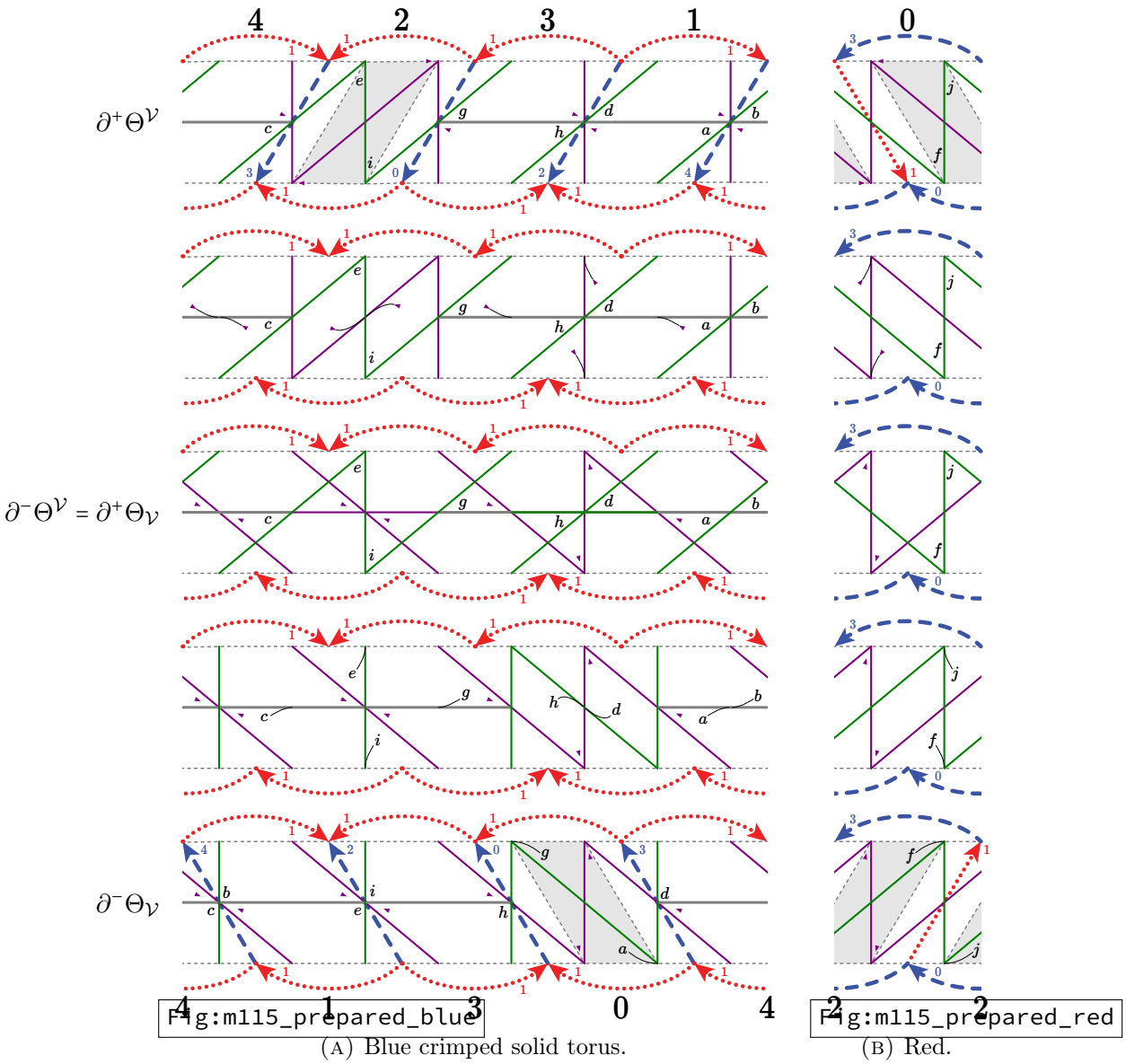

(A) Blue crimped solid torus. (B) Red.

FIGURE 8.2. The intersection of $B^{\mathcal{V}}$ (and $B_{\mathcal{V}}$), after parting, with various cross-sections of the crimped shearing decomposition of `fLLQccecddehqrwjj_20102`. Again, and as in Figure 7.13, the branched surface $B^{\mathcal{V}}$ is almost vertical in $\Theta^{\mathcal{V}}$ while $B_{\mathcal{V}}$ is almost vertical in $\Theta_{\mathcal{V}}$.

Fig:m115_prepared

Θ^U we do the same, but now moving track-cusps until they almost meet the projection (in bigon coordinates) of the midpoint of a helical edge.

Rem:AlmostProduct *Remark* 8.4. Thus $B^{\mathcal{V}}$ is almost a product in $\Theta^{\mathcal{V}}$. (In $\Theta^{\mathcal{V}}$ track-cusps move very slowly forward to preserve dynamism.) ◇

Rem:UpGivesDown *Remark* 8.5. Since $\partial^+\Theta^{\mathcal{V}}$ is glued to $\partial^-\Theta_{\mathcal{V}}$ parted position in the former determines parted position in the latter. Parted position is thus determined in fan and toggle squares, as shown in Figure 8.6. For our running example this is shown in the bottom and top rows of Figure 8.2.

Note that the track-cusps are slightly off the edges. This is so that they can very slowly move (horizontally) as we move up or down through cross-sections. We do this to ensure dynamism. ◇

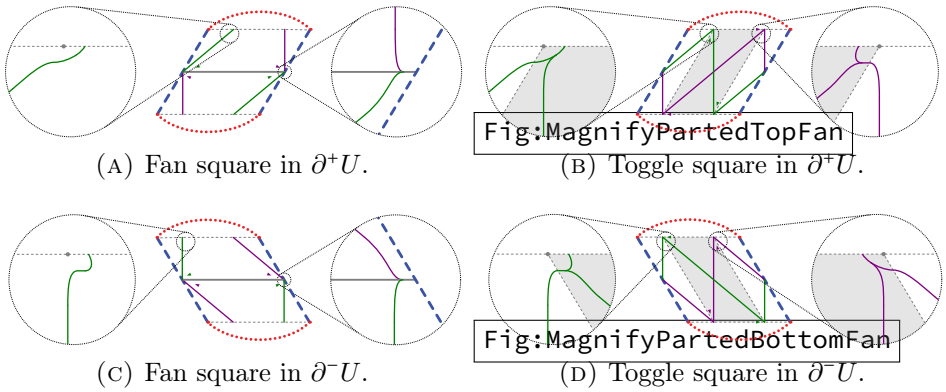

(A) Fan square in ∂^+U.

Fig:MagnifyPartedTopFan (B) Toggle square in ∂^+U. Fig:MagnifyPartedTopT

(C) Fan square in ∂^-U.

Fig:MagnifyPartedBottomFan (D) Toggle square in ∂^-U. Fig:MagnifyPartedBott

FIGURE 8.6. In prepared position the intersections of $B^{\mathcal{V}}$ and $B_{\mathcal{V}}$ with cross-sections are straight lines except for inside of the stations and very close to the midpoints of helical edges. In stations, branches meeting longitudinal crimped edges have the same tangent as the adjacent helical crimped edge. Fig:MagnifyParted Note that here U, the containing crimped shearing region, is blue.

Def:Graphical **Definition 8.7.** Suppose that U is a crimped shearing region. Suppose that H is a cross-section in U. Suppose that α is a smooth arc in H. We say that α is *graphical* if its tangent vectors (including at its endpoints) have non-zero x–coordinate. That is, α is transverse to the foliation U by bigons.

Suppose that τ is a train track in H. We say that τ is *graphical* if all of its branches are graphical. ◇

We will use the following lemma several times, in this section and the next.

gPreservesGraphical **Lemma 8.8.** *Suppose that τ is a graphical train track. Suppose that α is a train route in τ. Then the result of splitting τ along α is again graphical.* □

m:UpPartedGraphical

Lemma 8.9. *Suppose that H is any cross-section in $\Theta^{\mathcal{V}}$. The parted position of $B^{\mathcal{V}}$ in H is a train track for which all branches are graphical.*

The same is true for the parted position of $B^{\mathcal{V}}$ in $\partial^-\Theta_{\mathcal{V}}$ except for those branches which are in a platform in $\partial^-\Theta_{\mathcal{V}}$ meeting a longitudinal crimped edge. It follows that any train route in $\partial^-\Theta_{\mathcal{V}}$ avoiding these branches is graphical.

Proof. Suppose that U is a crimped shearing region. As discussed in Section 8.3, prepared position in Θ^U is defined locally. From Figure 8.12 we see that all branches of the tracks (outside of the stations) are straight. Note that some branches appear to be parallel to the y-axis; however, those actually have slightly positive slope. This is due to our choice of location for the corners of the toggle squares (made in Remark 6.2(2)). Thus all branches of the tracks are graphical.

The track inside of the stations, in both ∂^+U and ∂^-U, are laid out according to Figure 8.6. □

Sec:PartingDown

8.10. **Parting in $\Theta_{\mathcal{V}}$.** The parting isotopy in $\Theta_{\mathcal{V}}$ is more delicate. Here we introduce the definitions of a *neighbourhood splitting* and a *graphical isotopy*.

Sec:PartingRoutes

8.10.1. *Parting routes.*

Def:PartingRoutes

Definition 8.11. Suppose that U is a crimped shearing region. Suppose that K is a branch line of $B^{\mathcal{V}}$ (before parting) meeting U. Let k_0 and k_1 be the intersections of K with ∂^-U and ∂^+U respectively. Let k_1' be the projection of k_1 (under bigon coordinates) to ∂^-U. In a slight abuse of notation, we use the same names for the corresponding track-cusps (and projection) in ∂^-U and ∂^+U after parting (as in Section 8.3). Then the *parting route* $\alpha(k_0)$ is the unique route from k_0 to k_1' carried by the parted track in ∂^-U. ◇

Since the parting isotopy in $\Theta^{\mathcal{V}}$ is local, there are only a small number (in fact six) combinatorial possibilities for $\alpha(k_0)$. These are all shown in Figure 8.12.

- Suppose that k_1 lies in a toggle square in ∂^+U.
  - If k_0 also lies in a toggle square (in ∂^-U) then we obtain the examples f and j in Figure 8.12B.
  - Otherwise k_0 does not lie in a toggle square and we obtain the examples e and i in Figure 8.12A.
- Suppose that k_1 does not lie in a toggle square.
  - Suppose that k_1' lies in a toggle square.
    - If k_0 lies in a toggle square then we obtain the examples shown in Figure 8.12C.

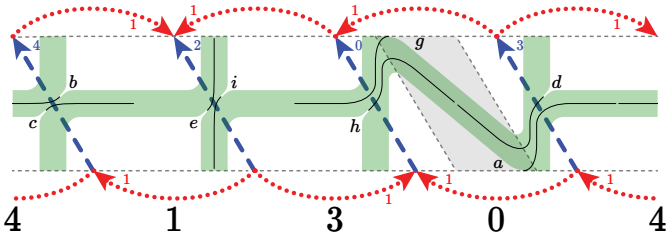

(A) Blue crimped solid torus.

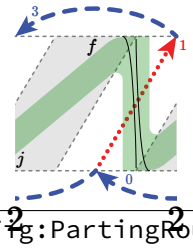

Fig:PartingRoutesBlue Fig:PartingRoutesRed

(B) Red.

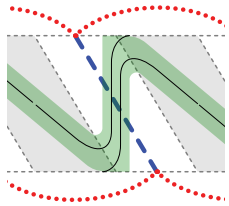

Fig:PartingRoutesSixth

(C) The sixth case.

FIGURE 8.12. Parting routes for the track-cusps in $\partial^- \Theta_{\mathcal{V}}$, where $\mathcal{V}$ is `fLLQccecddehqrwjj_20102`. Here we draw a regular neighbourhood of the train track in green.

Fig:PartingRoutes

- Otherwise k_0 does not lie in a toggle square and we obtain the examples d and h in Figure 8.12A.
- Suppose that k_1' does not lie in a toggle square.
  - If k_0 lies in a toggle square then we obtain the examples a and g in Figure 8.12A.
  - Otherwise k_0 does not lie in a toggle square and we obtain the examples b and c in Figure 8.12A.

dSplittingInParting

8.12.2. *Neighbourhood splitting.* Suppose that U is a crimped shearing region. Let H_s be the family of cross-sections of Θ_U, with $H_0 = \partial^- \Theta_U$ and $H_1 = \partial^+ \Theta_U$. Recall that $B^{\mathcal{V}}$ in parted position is already specified in H_0 and H_1. Instead of parametrising the parting isotopy explicitly, we specify parted position in $H_s \cap B^{\mathcal{V}}$ by giving a family of train tracks.

As s ranges over $[0, 1/2]$ the intersections of $B^{\mathcal{V}}$ (in parted position) with the cross-sections H_s show a movie of a splitting. In detail: if k is a track-cusp in H_0 we split k forward in a small neighbourhood of its parting route $\alpha(k)$. The result in one example is shown in the lower three rows of Figure 8.1. When two track-cusps k and ℓ meet, travelling in opposite directions, they split past each other. (If U is blue and there is (not) a toggle square above, this is a left (right) split. If U is red the directions swap.) Each track-cusp moves so that

- its x–coordinate moves at constant speed and
- its journey takes all of $[0, 1/2]$.

As a consequence of the construction given in Definition 8.11, track-cusps in $H_{1/2}$ lie either on the centre line of the cross-section, or in platforms. See the middle row of Figure 8.1.

In addition, for branches which meet longitudinal crimped edges, we shear the tangent vector where they meet. We do this twice as fast as in Remark 7.14. This ensures that, in $H_{1/2}$, the tangent vector has the same slope as the helical edges in $\partial^+ U$.

This describes the *neighbourhood splitting*.

dwayPartedGraphical

Remark 8.13. Let $\tau^{1/2}$ be the resulting train track in $H_{1/2}$. The shearing described above and Lemmas 8.8 and 8.9 ensure that all branches of $\tau^{1/2}$ are graphical.

Let τ^1 be the train track in $H_1 = \partial^+ \Theta_U = \partial^- \Theta^U$. By Remark 8.4, the train track τ^1 is a very small folding of the train track in $\partial^+ \Theta^U$. By Lemma 8.9, the train track τ^1 is also graphical. ◇

calIsotopyInParting

8.13.3. *The graphical isotopy.* For $s \in [1/2, 1]$, we perform a *graphical isotopy* from $\tau^{1/2}$ to τ^1, as follows. By Remark 8.13, both train tracks are graphical and they are combinatorially isomorphic. Also their track-cusps are in (almost) the same places in bigon coordinates. For each point of each branch of $\tau^{1/2}$, we change its y-coordinate at constant speed, from its initial position in $\tau^{1/2}$ to its final position in τ^1. We also very slightly move track-cusps forward to maintain dynamicism. This describes the *graphical isotopy*.

See the upper three rows of Figure 8.1.

dIsotopicAndDynami

Lemma 8.14. *The result of the parting isotopy in $\Theta^{\mathcal{V}}$ glued to the branched surface in $\Theta_{\mathcal{V}}$, produced by the neighbourhood splitting and graphical isotopy, is dynamic and is isotopic to $B^{\mathcal{V}}$ after shrinking.*

Proof. The intersection of this branched surface with each cross-section is a train track. Moreover, by construction the track-cusps always move forwards as we move up through cross-sections. Therefore the branched surface is dynamic.

In Section 8.3 we explicitly describe an isotopy between the shrunken branched surface and the parted branched surface in $\Theta^{\mathcal{V}}$. Thus in $\Theta_{\mathcal{V}}$ the shrunken branched surface and the constructed branched surface meet $\partial^- \Theta_{\mathcal{V}}$ and $\partial^+ \Theta_{\mathcal{V}}$ with the same combinatorics. It follows that the constructed branched surface is isotopic to the shrunken branched surface. □

We call the result *prepared position* for $B^{\mathcal{V}}$. We define the lower preparatory isotopy of the lower branched surface $B_{\mathcal{V}}$ analogously.

8.15. **Splitting routes.** From now it will be convenient to work in the universal cover, rather than in M itself. Since our constructions are natural, they are automatically equivariant. In a slight abuse of notation we use the notation $B^{\mathcal{V}}$ instead of the more correct $\widetilde{B}^{\mathcal{V}}$. The splitting isotopies given in the next section are similar to the parting isotopies described above, but with two important changes. First, the motion of the parting isotopies through space is replaced by the motion of the splitting isotopies through time. Second, the parting routes are replaced by the *splitting routes*, which we now describe.

Def:SplittingRoute

Definition 8.16. Suppose that $B^{\mathcal{V}}$ is in parted position. Suppose that $c = c_0$ is a point of a branch line C. Starting at c_0, we follow C upwards until it meets, for the first time, a toggle square $S = S(c)$. (This exists by Lemma 2.10.) Let U be the crimped shearing region meeting and immediately below S. Let $H_1 = \partial^+ U$. We define $c_1 = C \cap H_1$. Let $\beta(c_1)$ be the train route with length zero carried by $B^{\mathcal{V}} \cap H_1$ which starts and ends at c_1. Since $\beta(c_1)$ has length zero, it consists of a tangent vector which points at the crimped edge of S which is longitudinal for U. Note that c_1, and thus $\beta(c_1)$, is contained in the intersection of S and a platform centred at some corner of S. For an example, see the picture of the station (meeting $B^{\mathcal{V}}$ in green) in Figure 8.6B.

We parametrise the subinterval $[c_0, c_1]$ of C by $[0,1]$. Fix s and t in $[0,1]$ with $s < t$. Let $[c_s, c_t] \subset [c_0, c_1]$ be the corresponding subinterval. Suppose that $[c_s, c_t]$ is contained inside a crimped shearing region U. There are now two cases as c_s lies in the interior of, or lies in the lower boundary of, U.

First suppose that c_s is in the interior of U. Let H_s (H_t) be the cross-section of U through c_s (c_t). Suppose that the train route $\beta(c_t)$, carried by $B^{\mathcal{V}} \cap H_t$, is given. We are given that $\beta(c_t)$ runs from c_t to a point inside of a station at the boundary of H_t. We then form the train route $\beta(c_s)$, carried by $B^{\mathcal{V}} \cap H_s$, as follows. The start of $\beta(c_s)$ is $c_s \in C$. The end of $\beta(c_s)$ is the projection (in bigon coordinates) of the end of $\beta(c_t)$. Note that the end of $\beta(c_s)$ is again a point in a station.

Suppose instead that c_s lies in the lower boundary of U. We form $\beta'(c_s)$ by following the procedure given in the previous paragraph. If $\beta'(c_s)$ does not meet any toggle squares then we set $\beta(c_s) = \beta'(c_s)$ and note that the end point of $\beta(c_s)$ lies inside of the same station as $\beta(c_t)$. If $\beta'(c_s)$ does meet a toggle square, then we *truncate*: we delete from $\beta'(c_s)$ all intersections with toggle squares and keep only the segment meeting c_s, to obtain $\beta(c_s)$. In this case $\beta(c_s)$ ends on a helical crimped edge, inside the yard of some (possibly different) station. See Figure 8.6D.

We define $\beta(c) = \beta(c_0)$. This is the *splitting route* for c. $\diamond$

From their construction, we have that $\beta(c)$ is a train route in all cross-sections containing c. In each it runs from c to a point in a station. See Figure 8.17. When c is in a toggle square, $\beta(c)$ is completely contained in the platform, inside the station, and also within the toggle square.

ittingRoutesNoCross **Lemma 8.18.** *Suppose that H is any cross-section. Suppose that c and d are track cusps of $B^{\mathcal{V}} \cap H$. Then $\beta(c)$ and $\beta(d)$ do not* cross*: that is, after a small motion of $\beta(c)$ the two routes are disjoint.*

Proof. We use the notation of Definition 8.16. Let $[c_0, c_1]$ and $[d_0, d_1]$ be the resulting branch intervals in the branch lines C and D containing c and d respectively. Let c_s and d_t be the last points in these branch intervals for which there is a horizontal cross-section H' containing both. We deduce that H' is the upper boundary of some crimped shearing region U.

Claim 8.19. $\beta(c_s)$ and $\beta(d_t)$ are disjoint, thus they do not cross.

Proof. If $s = 1$ then $\beta(c_s)$ is contained in a station. In this case, if $\beta(d_t)$ meets $\beta(c_s)$ then (due to the truncation step of the construction) we find that $\beta(c_s) = \beta(d_t)$. Thus $c_0 = d_0$ and we are done.

A similar proof deals with the case that $t = 1$. We may now suppose that $s < 1$ and $t < 1$. Let T' be the union of the toggle squares of H'. Define $H'' = H' - T'$. Note that each component of H'' also appears as a subsurface of the lower boundary of some crimped shearing region. Since c_s and d_t are the last points of $[c_0, c_1]$ and $[d_0, d_1]$ in a common cross-section, we find that c_s and d_t are necessarily in different components of H''. By construction $\beta(c_s)$ and $\beta(d_t)$ are also contained in these components, so are disjoint. $\square$

We now reparameterise $[c_0, c_s]$ and $[d_0, d_t]$ by the unit interval and rechoose our notation so that, for all $r \in [0, 1]$, the track-cusps c_r and d_r lie in the same cross-section H_r. By the claim, when $r = 1$ the routes $\beta(c_r)$ and $\beta(d_r)$ are disjoint in H_r. Let $\tau^r = B^{\mathcal{V}} \cap H_r$. The tracks τ^r *fold* as r decreases. Folding preserves the property of not crossing, and we are done. $\square$

9. The splitting isotopy

Sec:Splitting

Suppose that the upper and lower branched surfaces $B^{\mathcal{V}}$ and $B_{\mathcal{V}}$ are in prepared position. From this point on, our isotopies are fixed on the union of the toggle squares. That is, each isotopy is supported

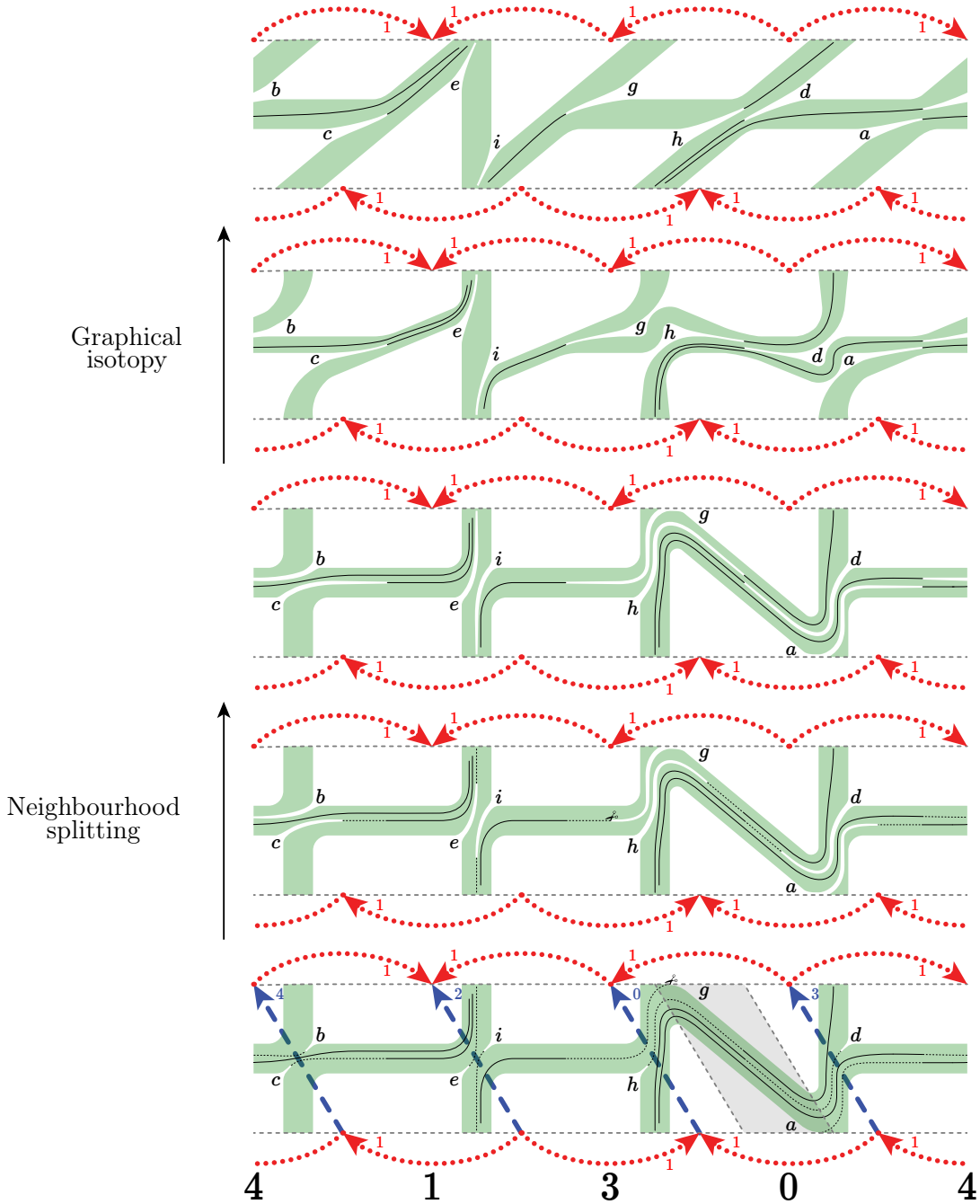

FIGURE 8.17. Splitting routes $\beta(a)$ through $\beta(i)$ for the track-cusps in cross-sections of Θ_U, where U is the blue crimped solid torus of `fLLQccecddehqrwjj_20102`. Compare with Figure 8.1A. For each splitting route, the subcurve which is the corresponding parting route is drawn with a dotted line.

Fig:SplittingRoutes

in the interiors of the red and blue parts of the crimped shearing decomposition.

We now describe the *upper* and *lower splitting isotopies* of $B^{\mathcal{V}}$ and $B_{\mathcal{V}}$ respectively. These move $B^{\mathcal{V}}$ downwards and $B_{\mathcal{V}}$ upwards. The isotopies get their name from how the moving branched surfaces meet a fixed cross-section H; the intersection is a splitting sequence of train tracks in H.

We use $B^{\mathcal{V}}_t$ to denote the image of $B^{\mathcal{V}}$ at time $t \in [0,1]$. It now suffices, for each cross-section H, to

- describe the intersection $B^{\mathcal{V}}_t \cap H$ and
- check that the descriptions depend continuously on the choice of H.

gIsotopyMiddleUpper

9.1. **The upper splitting isotopy in $\Theta^{\mathcal{V}}$.**

plittingInSplitting

9.1.1. *Neighbourhood splitting.* For $t \in [0, 1/2]$, we do the following. Suppose that H is a horizontal cross-section in $\Theta^{\mathcal{V}}$ and suppose that $c \in B^{\mathcal{V}} \cap H$ is a track-cusp. We split c forward in a small neighbourhood of its splitting route $\beta(c)$ until we reach the station containing the end of $\beta(c)$. For an example of the overall motion of the track-cusps see the lower three rows of Figure 9.2.

Applying Lemma 8.18, when two track-cusps c and d meet travelling in opposite directions, they split past each other, splitting to the left or right as determined by the combinatorics of their splitting routes. Each track-cusp moves at the constant speed required for its journey to take all of $[0, 1/2]$. This and Lemma 8.18 ensure that track-cusps travelling in the same direction never meet.

The construction in Definition 8.16 ensures that when a track-cusp c enters a station it moves all the way to the platform (in the projection of $S(c)$) if there is no track-cusp already there. The track-cusp c then points at e', a longitudinal edge for the ambient crimped shearing region. See the picture of the station in Figure 9.2.

When a track-cusp c enters a station, and there is a track-cusp d already at the platform, then c only enters the yard. Furthermore, c remains outside of the projection of $S(d)$, pointing at the projection of its helical crimped edge. The construction in Definition 8.16 ensures that when multiple track-cusps arrive to the same station (and the platform is occupied) they line up in the yard, in order of their appearance. Again, see the picture of the station in Figure 9.2.

This describes the *neighbourhood splitting.*

lIsotopyInSplitting

9.1.2. *The graphical isotopy.* For $t \in [1/2, 1]$, we do the following. Suppose that b is a branch of $B^{\mathcal{V}}_{1/2} \cap H$. Note that the endpoints of b lie

inside of stations. Also note that by Lemmas 8.8 and 8.9, the branch b is graphical. We isotope so that, at $t = 1$, all branches of the train track are straight lines in bigon coordinates, other than in the stations. For each point of each branch, we change only its y-coordinate in bigon coordinates, moving at constant speed from its initial to its final position. This describes the *graphical isotopy*. See the upper three rows of Figure 9.2.

em:UpGivesDownAgain *Remark* 9.3. As in Remark 8.5, the intersection of the image of the upper splitting isotopy with cross-sections in $\Theta^{\mathcal{V}}$ determines the intersection of the image of the upper splitting isotopy with $\partial^{-}\Theta_{\mathcal{V}}$. ◇

littingIsotopyLower 9.5. **The upper splitting isotopy in $\Theta_{\mathcal{V}}$.** Fix U, a blue crimped shearing region. We use H_s to denote the cross-section of Θ_U at height $s \in [0,1]$. (This matches the values for s given in the captions for Figures 9.2, 9.4, and 9.8.) It remains to describe the intersections $B_t^{\mathcal{V}} \cap H_s$. The intersections $B_0^{\mathcal{V}} \cap H_s$ are given by the preparatory isotopy. Also, $B_t^{\mathcal{V}} \cap H_1$ and (by Remark 9.3) $B_t^{\mathcal{V}} \cap H_0$ are already determined by the splitting and isotopy given in Section 9.1. This gives three sides of the "boundary of the isotopy". We now describe the fourth; that is, we describe $B_1^{\mathcal{V}} \cap H_s$ for $s \in [0,1]$.

9.5.1. *Suffix routes.* We wish to define the *suffix routes* for track-cusps of $B_1^{\mathcal{V}} \cap H_0$.

Def:SuffixRoutes **Definition 9.6.** Suppose that k is a track-cusp of $B_1^{\mathcal{V}} \cap H_0$. Following our construction backwards, k is the endpoint of a splitting route $\beta(k')$ starting at k' and carried by $B_0^{\mathcal{V}} \cap H_0$. Suppose that ℓ' is the track-cusp of $B_0^{\mathcal{V}} \cap H_1$ on the same branch interval of $B_0^{\mathcal{V}} \cap U$ as k'. Let ℓ be the endpoint of the splitting route $\beta(\ell')$ starting at ℓ' and carried by $B_0^{\mathcal{V}} \cap H_1$.

Let $\beta'(\ell') \subset B_0^{\mathcal{V}} \cap H_0$ be the result of folding $\beta(\ell')$ downward through $B_0^{\mathcal{V}} \cap U$. By construction, $\beta(k')$ is obtained from $\beta'(\ell')$ by removing any intersection with toggle squares in $\partial^{-}U$ and taking the initial segment. Define $\gamma'(k') = \beta'(\ell') - \beta(k')$. Note that this is a train route in $B_0^{\mathcal{V}} \cap H_0$. By construction and by Lemma 8.18 none of the splitting routes in $B_0^{\mathcal{V}} \cap H_0$ cross $\gamma'(k')$. We take the image of $\gamma'(k')$ under the neighbourhood splitting and graphical isotopy defined in Section 9.1. The result is the *suffix route* $\gamma(k)$ which starts at k, is carried by $B_1^{\mathcal{V}} \cap H_0$, and which ends at (the projection in bigon coordinates of) ℓ. ◇

Claim 9.7. The suffix route $\gamma(c)$ is carried by the graphical subtrack of $B_1^{\mathcal{V}} \cap H_0$ and so is graphical.

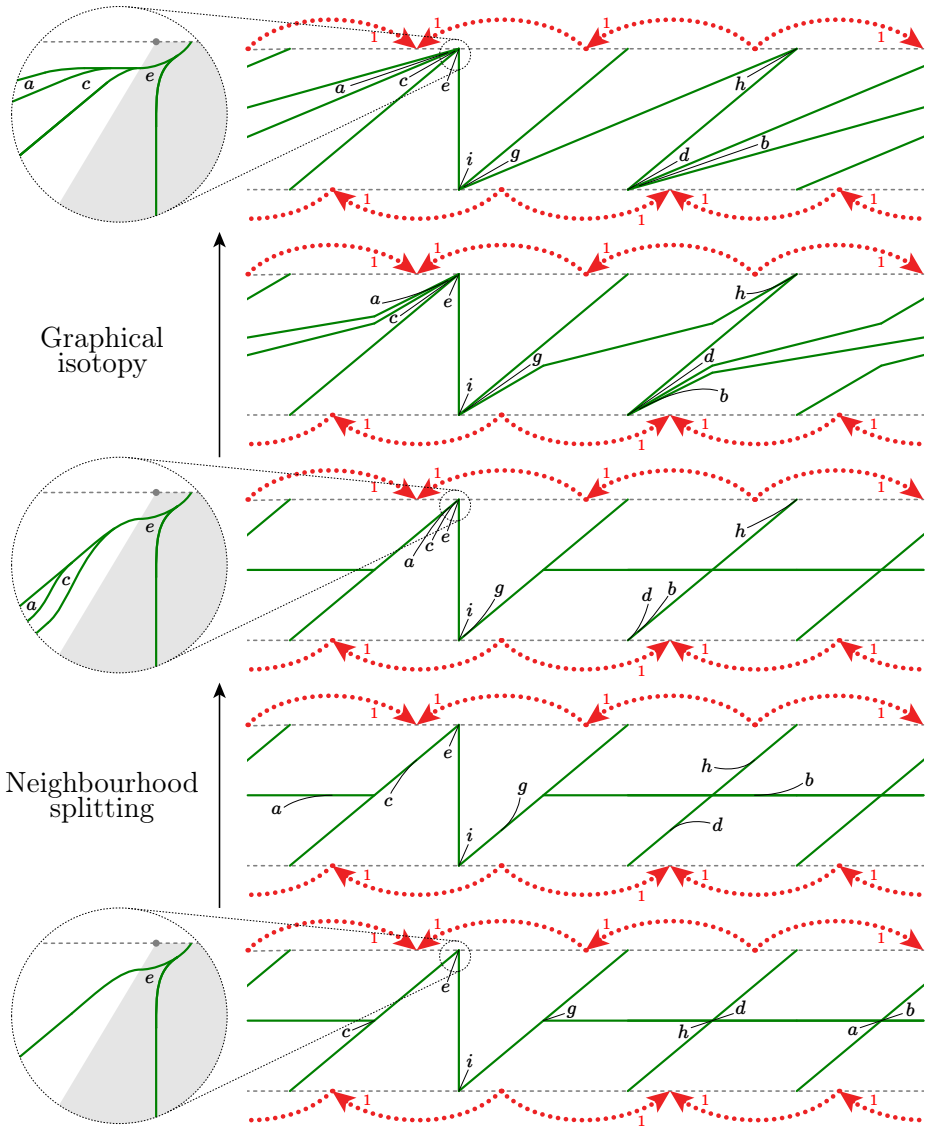

FIGURE 9.2. The splitting isotopy for the cross-section $\partial^- \Theta^{\mathcal{V}} = \partial^+ \Theta_{\mathcal{V}}$ at the middle of U, $(s = 1)$. Here U is the blue crimped solid torus for `fLLQccecddehqrwjj_20102`. Note that, as shown in the close-up views of a station, track-cusps never touch. The close-up views also show the projection under bigon coordinates of the toggle square $S(e)$ (as in Definition 8.16) above the station.

ence_top_of_Omega_V

Proof. Recall that $H_0 = \partial^- U$. Again by Lemmas 8.8 and 8.9, the train track $B_1^{\mathcal{V}} \cap H_0$ is graphical except for those branches which are in a platform in $\partial^- \Theta_{\mathcal{V}}$ meeting a longitudinal crimped edge. The

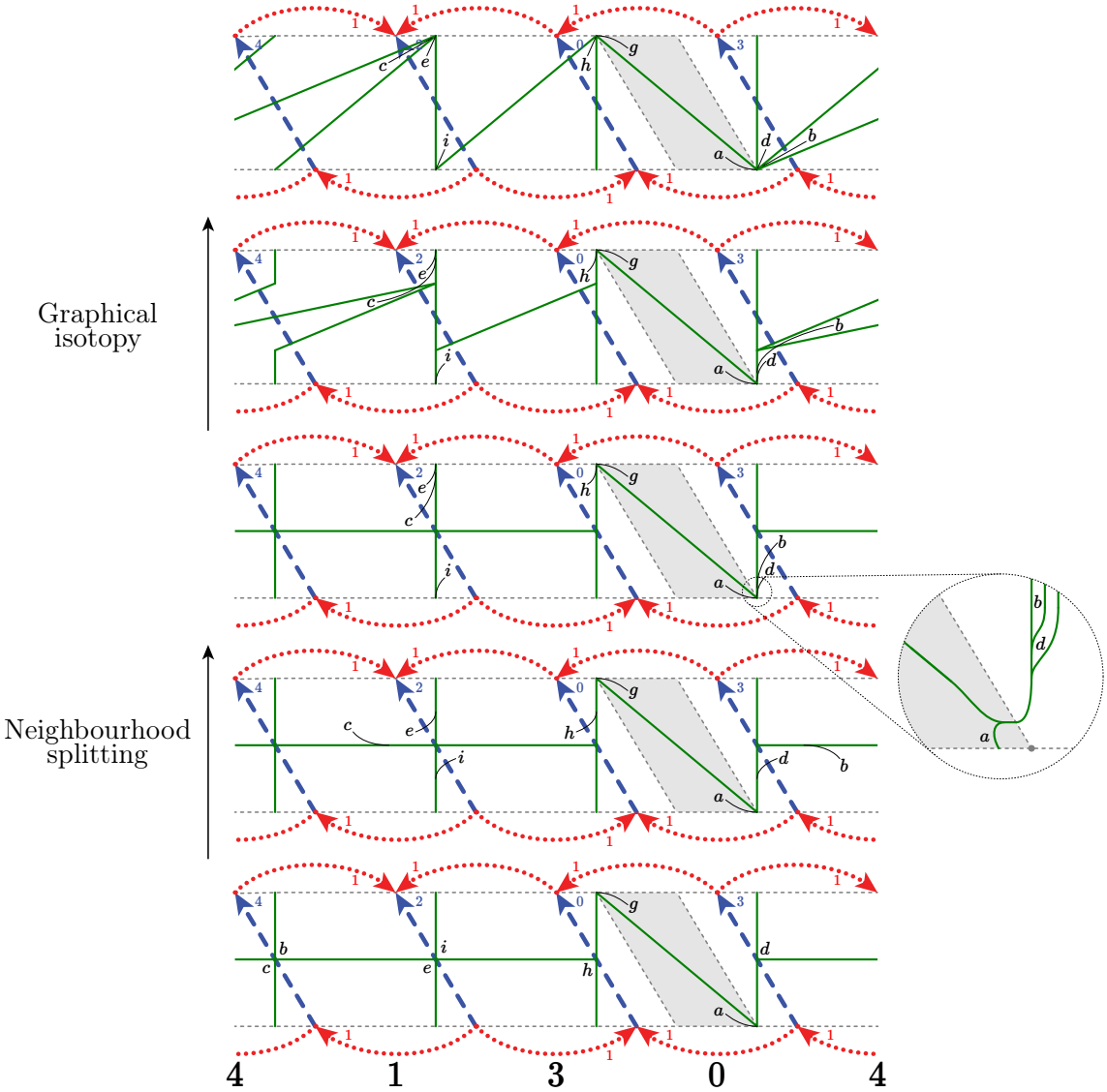

FIGURE 9.4. The splitting isotopy for the cross-section at the bottom of Θ_U ($s = 0$), where U is the blue crimped solid torus for `fLLQccecddehqrwjj_20102`.

e_bottom_of_Omega_V

splitting route $\beta(\ell')$ does not meet such a branch (Definition 8.16). Therefore neither does its fold $\beta'(\ell')$, and so neither does the route $\gamma'(k)$. The neighbourhood splitting and graphical isotopy do not alter this (Lemma 8.8). $\square$

As in Section 8.12.2, we now perform a neighbourhood splitting (in space), replacing the parting routes α by the remaining routes γ. As s progresses through $[0, 1/2]$ we split a track-cusp c forward along $\gamma(c)$.

We now perform (in space) a graphical isotopy, analogous to the one described in Section 8.13.3. As s progresses through $[1/2, 1]$, we graphically straighten the branches. As usual, the track-cusps move very slowly forwards to ensure dynamism. See Figure 9.8.

Now that the four sides of the isotopy are given, we fill in the interior. That is, we must describe the train-tracks $B_t^{\mathcal{V}} \cap H_s$ for $s, t \in (0, 1)$. As usual, we begin by finding the routes needed for the neighbourhood splitting.

9.8.2. *Prefix routes.*

Def:PrefixRoutes **Definition 9.9.** Suppose that s lies in $[0, 1]$. Let k be a track-cusp in $B_0^{\mathcal{V}} \cap H_s$. Let ℓ be the track-cusp in $B_0^{\mathcal{V}} \cap H_1$ which is on the same branch interval (of $B_0^{\mathcal{V}}$) as k. Let ℓ' be the endpoint of the route $\beta(\ell)$. Let k' be the track-cusp in $B_1^{\mathcal{V}} \cap H_s$ which is on the same branch interval (of $B_1^{\mathcal{V}}$) as ℓ'.

We define the *prefix route* $\delta(k)$ to be the prefix of $\beta(k)$ which ends at the point of $\beta(k)$ with the same x–coordinate as k'. $\diamond$

For each fixed s, we perform the neighbourhood splitting (for $t \in [0, 1/2]$) and graphical isotopy (for $t \in [1/2, 1]$). During the neighbourhood splitting, each track-cusp moves from its position in $B_0^{\mathcal{V}} \cap H_s$ to its position in $B_1^{\mathcal{V}} \cap H_s$.

This completes the definition of the upper splitting isotopy. The lower splitting isotopy of $B_{\mathcal{V}}$ is defined analogously, with the roles of Θ^U and Θ_U reversed. Note that both the upper and lower splitting isotopies are continuous by construction.

We apply the splitting isotopies to $B^{\mathcal{V}}$ and $B_{\mathcal{V}}$ beginning from prepared position. We call the result *split position.* For examples, see Figures 9.11 and 9.12.

9.10. **Split position.** We make the following observations.

em:SplittingDynamic **Lemma 9.13.** *In split position, the branched surfaces $B^{\mathcal{V}}$ and $B_{\mathcal{V}}$ are dynamic.*

Proof. In split position the branched surface $B^{\mathcal{V}}$ is transverse to the cross-sections of all crimped shearing regions. Furthermore, we have arranged that track-cusps always move forwards as we move up through cross-sections. The same argument applies to the lower splitting isotopy, acting on $B_{\mathcal{V}}$. $\square$

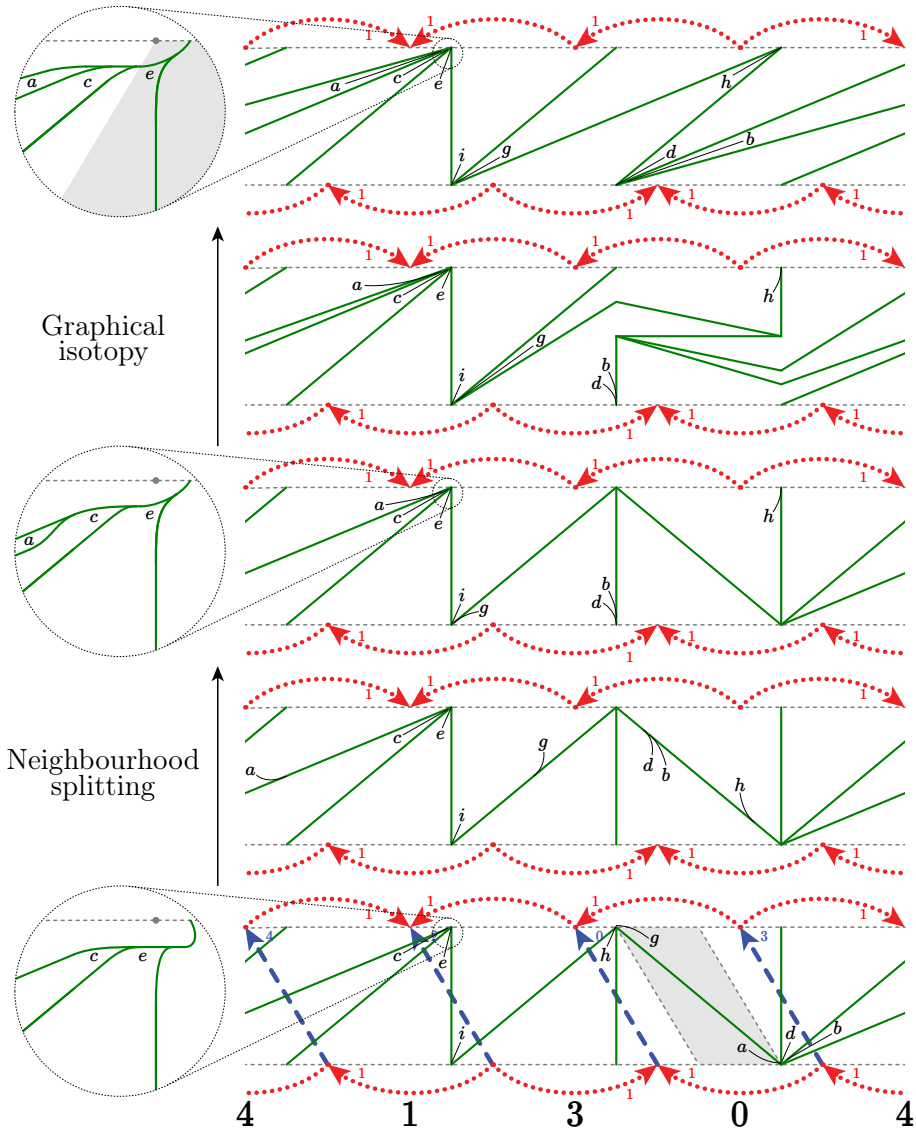

FIGURE 9.8. The result $B_1^{\mathcal{V}}$ of the splitting isotopy in Θ_U where U is the blue crimped solid torus for `fLLQccecddehqrwjj_20102`. The five diagrams show (from the bottom moving up) $B_1^{\mathcal{V}} \cap H_s$ for $s \in (0, 1/4, 1/2, 3/4, 1)$. The bottom cross-section contains blue helical edges. In the uppermost magnifying glass we have also drawn the (projection in bigon coordinates) of the upper toggle square.

tting_sequence_blue

Lem:TrackCuspNoGo

Lemma 9.14. *Suppose that G and H are cross-sections in Θ^U with G above H. Then with $B^{\mathcal{V}}$ in split position, the projection of τ^G to H in*

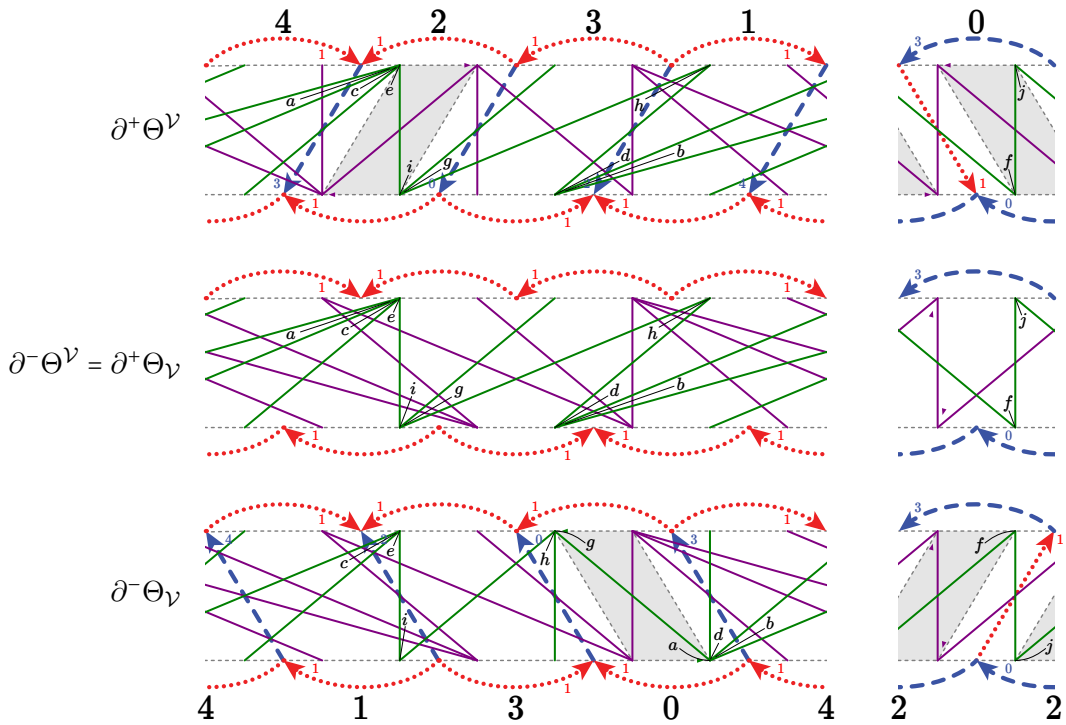

(A) Blue crimped solid torus. (B) Red.

FIGURE 9.11. The intersection of $B^{\mathcal{V}}$ (and $B_{\mathcal{V}}$), in split position, with various cross-sections of the crimped shearing decomposition of `fLLQccecddehqrwjj_20102`. Compare with Figure 8.2.

Fig:m115_split

bigon coordinates is carried by, and is up to a small isotopy equal to, τ^H. The same holds for $B_{\mathcal{V}}$ in Θ_U.

Proof. Let τ_t^G be the intersection of G and $B_t^{\mathcal{V}}$. Define τ_t^H similarly. Suppose that C is the branch line through track-cusps c of τ_0^G and d of τ_0^H. Following the construction given in Section 9.1, we obtain train routes $\beta(c) \subset \tau_0^G$ and $\beta(d) \subset \tau_0^H$. Since there are no toggle squares strictly between G and H, the forward endpoint of $\beta(c)$ projects to the forward endpoint of $\beta(d)$. Thus after the neighbourhood and graphical isotopies, τ_1^G projects to τ_1^H (after moving the track-cusps of τ_1^H slightly forward). □

ryCrossSectionSplit

Lemma 9.15. *Suppose that $B^{\mathcal{V}}$ and $B_{\mathcal{V}}$ are in split position. Suppose that U is a blue shearing region. Suppose that H is either ∂^+U, the upper boundary of U, or ∂^-U, the lower boundary. Let $\tau^H = H \cap B^{\mathcal{V}}$ and $\tau_H = H \cap B_{\mathcal{V}}$.*

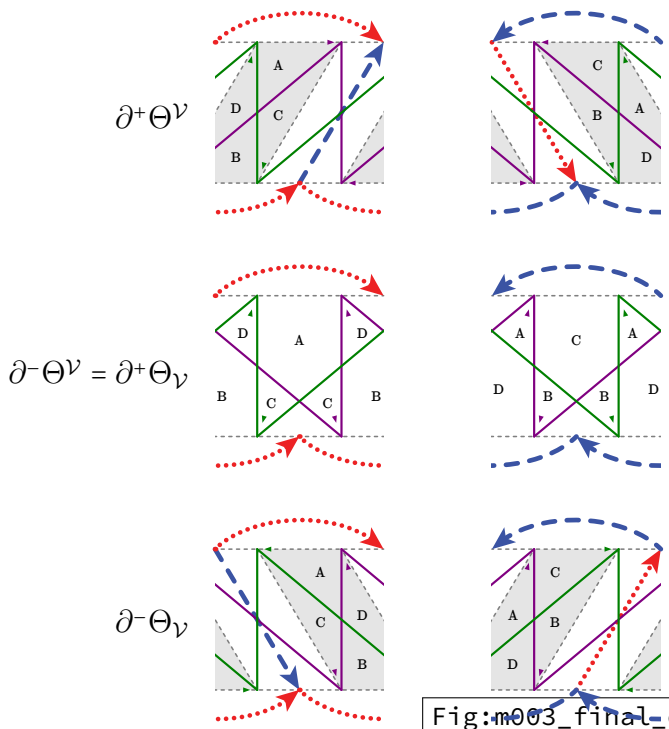

(A) Blue solid torus. (B) Red solid torus.

Fig:m003_final_cross-sections_blue Fig:m003_final_cross-sections_red

FIGURE 9.12. Split position for the figure-eight knot sibling with veering triangulation `cPcbbbdxm_10`. The four pinched tetrahedra are labelled A through D. To obtain the pictures for the figure-eight knot complement with veering triangulation `cPcbbbiht_12`, alter these figures by requiring that the orientation on every helical edge points upwards. (To relabel the pinched tetrahedra, start with those given at the top of Figure 9.12A and propagate outwards.)

PositionFig8Sibling

Itm:Straight

Itm:Slopes

:ToggleSquareSlopes

Itm:TrackCusp

:NextToToggleSquare

(1) *Outside of the stations, the branches of τ^H and τ_H are straight lines (in bigon coordinates).*
(2) *Outside of toggle squares, the branches of τ^H have strictly positive slope and the branches of τ_H have strictly negative slope.*
(3) *Inside of each toggle square, outside of the stations, there is exactly one branch of τ^H and exactly one branch of τ_H. These have strictly negative and strictly positive slope respectively.*
(4) *Each track-cusp is in a station.*
(5) *Suppose that e is a helical edge in H. Suppose that, of the two equatorial squares adjacent to e, at least one lies in a toggle tetrahedron. Then the stations of τ^H immediately adjacent to e*

are connected by a branch of τ^H. Similarly, the stations of τ_H are connected by a branch of τ_H.

Itm:OneCusp

(6) *Every component of $H - \tau^H$ contains exactly one track-cusp, and exactly one ideal vertex of U. The same holds for $H - \tau_H$.*

When U is a red shearing region, a similar statement holds, swapping the signs of slopes. □

We generalise Lemma 9.15(6) to other cross-sections as follows.

Prop:OneCusp

Proposition 9.16. *Suppose that U is a crimped shearing region. Let H be a cross-section of U. Then every component of $H - \tau^H$ contains exactly one track-cusp and exactly one ideal vertex of U. The same holds for $H - \tau_H$.*

Proof. The result holds for $H' = \partial^- U$ by Lemma 9.15(6). Moving upwards from H' to H we perform splittings and graphical isotopies. Neither of these changes the combinatorics of a region of $H - \tau^H$. □

rdCrossSectionSplit

Lemma 9.17. *Suppose that $B^{\mathcal{V}}$ and $B_{\mathcal{V}}$ are in split position. Suppose that U is a blue shearing region. Suppose that H is the lower boundary of $\Theta(U)$. Let $\tau^H = H \cap B^{\mathcal{V}}$ and $\tau_H = H \cap B_{\mathcal{V}}$.*

Itm:ThirdStraight

(1) *Outside of the stations, the branches of τ^H and τ_H are straight lines (in bigon coordinates).*

tm:ThirdGreenSlopes

(2) *The branches of τ^H have strictly positive slope.*

m:ThirdPurpleSlopes

(3) *Above each toggle square, outside of its stations, there is exactly one branch of τ_H. This branch has slope more positive than any branch of τ^H. The remaining branches of τ_H (not above toggle squares) have strictly negative slope.*

Itm:ThirdTrackCusp

(4) *Each track-cusp is in station.*

A similar statement holds for H the upper boundary of $\Theta(U)$. Finally, all of the above again holds, swapping slopes appropriately, when U is a red shearing region.

Proof. Let $G = \partial^+ U$. By Lemma 9.15, statements (1) and (4) hold for τ^G. Also, (2) holds except that the slopes of branches have the wrong sign inside of toggle squares. By Lemma 9.14, these properties are carried to τ^H, and the shearing within $\Theta(U)$ corrects the signs of the slopes of branches coming from toggle squares in G. To obtain (3), we start from the lower boundary $K = \partial^- U$, and again use Lemma 9.14 to carry properties of τ_K up to τ_H. Finally, note that the only branches of τ^H with slope more positive than the exceptional branches of τ_H do not lie above a toggle square. (They lie above exactly one helical edge.) □

Lem:SlopeNearCusp

Lemma 9.18. *Suppose that $B^{\mathcal{V}}$ and $B_{\mathcal{V}}$ are in split position. Suppose that U is a blue shearing region. Suppose that H is any cross-section of*

U. Let $\tau^H = H \cap B^{\mathcal{V}}$ and $\tau_H = H \cap B_{\mathcal{V}}$. Let c be a cusp of U. Let E be the component of $H - (\tau^H \cup \tau_H)$ meeting c. Then the branches of τ^H appearing in the boundary of E have positive slope; the branches of τ_H appearing in the boundary of E have negative slope. There is a similar statement for a red shearing region.

Proof. First let $H = \partial^- U$. By Lemma 9.15(2) and (3), the only branches of the incorrect slope are in toggle squares. Appealing to Lemma 9.15(5), such branches are separated from the cusp c by other branches. Examining the neighbourhood and graphical isotopies, the conclusion holds in general. □

m:SplitMeetsToggles

Lemma 9.19. *Each subray of each branch line of $B^{\mathcal{V}}$ and of $B_{\mathcal{V}}$, in split position, meets crimped shearing regions of both colours.*

Proof. This follows from Lemma 2.10 and the fact that our isotopies do not change combinatorics in toggle squares. □

10. The dynamic pair

Sec:DynamicPair

Thm:DynamicPair

Theorem 10.1. *Suppose that $\mathcal{V}$ is a transverse veering triangulation. In split position, the upper and lower branched surfaces $B^{\mathcal{V}}$ and $B_{\mathcal{V}}$ form a dynamic pair; this position is canonical. Furthermore, if $\mathcal{V}$ is finite then split position is produced algorithmically in polynomial time and the dynamic train track $B^{\mathcal{V}} \cap B_{\mathcal{V}}$ has at most a quadratic number of edges.*

The branched surfaces $B^{\mathcal{V}}$ and $B_{\mathcal{V}}$ are individually dynamic by Lemma 9.13. We now verify the hypotheses of Definition 4.9. Again, it will be convenient to work equivariantly in the universal cover.

10.2. **Transversality.** Let U be a crimped shearing region. Recall that $B^{\mathcal{V}}$ and $B_{\mathcal{V}}$ are now in split position.

Lemma 10.3. *Suppose that H is a cross-section of U. Then the train-tracks τ^H and τ_H are transverse.*

Proof. For $H = \partial^- U$, this follows from Lemma 9.15(2), (3), and (4).

Now suppose that H_s for $s \in [0,1]$ is a cross-section in Θ_U. Let $\tau^s = B^{\mathcal{V}} \cap H_s$ and let $\tau_s = B_{\mathcal{V}} \cap H_s$. The train-tracks τ^s perform the neighbourhood and then graphical isotopies as described in Section 9.5. Note that τ^0 and τ_0 are transverse by the previous paragraph. By Lemma 9.14, the train-tracks τ_s are all essentially the same in bigon coordinates. During the neighbourhood splitting (that is, for $s \in [0, 1/2]$), the track-cusps of τ^s split forward in a small neighbourhood of (the

projection of) τ^0. Thus the train-tracks τ^s and τ_s are transverse for $s \in [0, 1/2]$.

By Lemma 9.17, the train-tracks τ^1 and τ_1 are transverse. We now consider $s \in [1/2, 1]$. The graphical isotopy interpolates between $\tau^{1/2}$ and τ^1. Let b^s and c_s be branches of τ^s and τ_s respectively.

Claim. The branches b^s and c_s are transverse.

Proof. Let c_0 be the projection of c_s down to $\partial^- U$. Suppose that c_0 lies completely within a toggle square. If the projection of $b^{1/2}$ misses this toggle square then we are done. Otherwise let a^s be the linear segment of b^s which meets the toggle square. Since the isotopy is graphical, the slope of a^s is between that of $a^{1/2}$ and a^1. Applying Lemma 9.15(3) and Lemma 9.17(3) we find that the slope of c_s is bigger than that of a^s. We deduce that c_s is transverse to a^s and thus to b^s.

Suppose instead that c_0 is disjoint from the toggle squares. In this case the proof is similar, but easier. Now the slope of c_s is always negative by Lemma 9.17(3). Also, the slope of a^s is always positive by Lemma 9.15(2), by Lemma 9.17(2), and by appealing to the graphical isotopy. □

Let K be the lower boundary of $\Theta(U)$. By the claim (for $s = 1$), the tracks τ^K and τ_K intersect transversely. Thus by Lemma 9.14, the same holds for τ^H and τ_H for every cross-section H in $\Theta(U)$.

Swapping the roles of upper and lower and repeating the argument proves that τ^H and τ_H are transverse for every cross-section H in Θ^U. □

Lemma 10.4. *Each branch interval of $B^{\mathcal{V}}$ in U is transverse to $B_{\mathcal{V}}$, and conversely.*

Proof. It suffices to show that for each cross-section H, the track-cusps of τ^H and of τ_H are disjoint. By Lemma 9.14, in $\Theta_U \cup \Theta(U)$ the track-cusps of τ_H lie within small neighbourhoods of the endpoints of sidings of τ_H. The same holds for track-cusps of τ^H in $\Theta(U) \cup \Theta^U$. The track-cusps of τ^H remain away from the sidings of τ_H in the upper splitting isotopy in Θ_U. Similarly, the track-cusps of τ_H remain away from the sidings of τ^H in the lower splitting isotopy in Θ^U. □

We record the following.

Rem:TrackCuspsGo3 *Remark* 10.5. As H moves upwards, if a track-cusp of τ^H moves through τ_H, it does so going forwards. Similarly, whenever a track-cusp of τ_H moves through τ^H, it does so going backwards. ◇

The above lemmas, together with the remark, prove that $B^{\mathcal{V}}$ and $B_{\mathcal{V}}$ are transverse.

10.6. **Separation.** Recall from Remark 2.8 that both $B^{\mathcal{V}}$ and $B_{\mathcal{V}}$ are isotopic (ignoring the branching structure) to the dual two-skeleton of $\mathcal{V}$. Suppose that C and D are components of $M - (B^{\mathcal{V}} \cup B_{\mathcal{V}})$, each containing a cusp of M. Thus, by Proposition 9.16, each of C and D contains exactly one cusp of M. Suppose that F is a two-cell of the natural cell structure on $B^{\mathcal{V}} \cup B_{\mathcal{V}}$. Suppose that F meets C on one side and D on the other. Then we can find a proper arc dual to F, and thus disjoint from one of $B^{\mathcal{V}}$ or $B_{\mathcal{V}}$. This is a contradiction.

Sec:Components

10.7. **Components.** We must show that every component C of $M - (B^{\mathcal{V}} \cup B_{\mathcal{V}})$ is either a dynamic shell or a pinched tetrahedron.

10.7.1. *Dynamic shell.* Suppose first that C contains one (thus by Proposition 9.16, exactly one) cusp c of M. Let v be a model of c where v is an ideal vertex of a red crimped shearing region U. Let $E = E(v, U)$ be the component of $U - (B^{\mathcal{V}} \cup B_{\mathcal{V}})$ incident to v. Our goal now is to prove the following.

- E is a three-ball,
- the frontier of E in U consists of two vertical "half-bigons" (one from each of $B^{\mathcal{V}}$ and $B_{\mathcal{V}}$),
- the boundary of E in $\partial^+ U$ consists of two triangular faces, both meeting a single helical edge of $\partial^+ U$, and
- the boundary of E in $\partial^- U$ consists of two triangular faces, both meeting a single helical edge of $\partial^- U$.

Fix a cross-section H of U. Looking into H from the vertex v, we see a siding of τ_H meeting the boundary of H to our left and a siding of τ^H meeting the boundary of H to our right. Appealing Lemma 9.18, the frontier of $H \cap E$ consists of branches of τ^H and τ_H intersecting precisely once. Stacking the cross-sections together, shows that E is a three-ball with the desired properties.

A similar argument applies for a blue shearing region U. Here the half-bigon of $B^{\mathcal{V}}$ is to the left, and the half-bigon of $B_{\mathcal{V}}$ is to the right.

Taking the union of the three-balls $E(v, U)$, as v ranges of the models of c, gives C. The half-bigons glue to give the stable and unstable faces of C. Note that any one half-bigon meets only finitely many others because the edges of $\mathcal{V}$ have finite degrees. Therefore, the $E(v, U)$ glue together to form a dynamic shell.

10.7.2. *Pinched tetrahedron.* Suppose instead that the component C does not contain any cusp c of M. We must show that C is a pinched tetrahedron. To show this, we will need the following definition and lemma.

xtendedCrossSectio

Definition 10.8. Suppose that $H \subset U$ is a cross-section. We define the *bigon extension* $\overset{\smile}{H}$ as follows. The boundary of H consists of some number of longitudinal crimped edges. Each such edge e cobounds a crimped bigon B with a coloured edge e'. For each edge e we glue a new copy of B onto H to obtain $\overset{\smile}{H}$. ◇

Note that the bigon extension $\overset{\smile}{H}$ may contain many copies of the same crimped bigon. For example, Figure 8.2A shows several extended cross-sections, each extended with multiple copies of the two crimped bigons incident to the single red longitudinal edge. (Note however that in that figure we have not drawn the intersection of the branched surfaces with these crimped bigons.)

ahedraCrossSectio

Lemma 10.9. *Suppose that H is a cross-section of a crimped shearing region U, meeting C. Then each component of the intersection $C \cap \overset{\smile}{H}$ is either a trigon or a quadragon, as defined in Definition 4.5. Moreover, as H moves up through U, components change according to the sequence given in Definition 4.5.*

Proof. Suppose that U is a red crimped shearing region. Let $(H_t \mid t \in [0,1])$ be the cross-sections of U. Thus $H_0 = \partial^- U$.

Claim. Suppose that R is such a component of $C \cap \overset{\smile}{H}_0$. Then R is either a trigon or a quadragon.

Proof. First suppose that R is entirely contained within $H = H_0$. From the first four items of Lemma 9.15, the boundary of R consists of three or four branch lines from τ^H and τ_H. If there are four then they alternate between τ^H and τ_H and R is a quadragon. If there are three then two lie in the same train track and meet at a track-cusp. Thus R is a trigon.

Now suppose that R is not entirely contained within H. By Lemma 9.15(5), the component R meets a crimped bigon B and contains the midpoint of the crimped edge. The frontier of R in B consists of exactly one arc from each of τ^B and τ_B, meeting at a point. The claim now follows in a manner similar to the previous paragraph. □

More generally, suppose that the claim holds with H_t replacing H_0. Let $\tau^t = H_t \cap B^{\mathcal{V}}$ (green) and $\tau_t = H_t \cap B_{\mathcal{V}}$ (purple). Remark 10.5 tells us that as t increases, there are only two combinatorial changes:

(1) Track-cusps of τ^t move forwards through branches of τ_t.
(2) Track-cusps of τ_t move backwards through branches of τ^t.

The first move simultaneously creates a new green trigon and converts a green trigon into a quadragon. The second move simultaneously deletes a purple trigon, and converts a quadragon into a purple trigon. These

are both moves between stages in the life of a pinched tetrahedron, as given in Definition 4.5, as required. This proves Lemma 10.9. □

Suppose that C is a complementary component of $M - (B^{\mathcal{V}} \cup B_{\mathcal{V}})$ which does not contain a cusp of M. We now show that the cross-sections that meet C undergo the above moves, and thus C is a pinched tetrahedron.

Let H be a cross-section through a crimped shearing region U, and let R be a region of $\breve{H} - (B^{\mathcal{V}} \cup B_{\mathcal{V}})$. Using Proposition 9.16 twice, gives track-cusps s^{R} and s_{R} of τ^H and τ_H respectively, so that R is a subset of the component of $\breve{H} - \tau^H$ containing s^{R}, and is also a subset of the component of $\breve{H} - \tau_H$ containing s_{R}.

First suppose that R is a green trigon. Thus R contains s^{R}. We must show that this track-cusp eventually crosses a purple arc, turning R into a quadragon. By Lemma 9.19, moving up, (the branch line containing) s^{R} eventually enters the bottom of a crimped shearing region V through a toggle square. If the region R persists into $\partial^- V$, and is still a green trigon, then moving up through Θ_V, the track-cusp s^{R} splits forwards and hits the purple arc given by Lemma 9.15(5). This turns R into a quadragon.

Moving down instead of up, a similar argument shows that every green trigon is born at some point. Similar arguments also show that as we move up purple trigons eventually die, and that as we move down, purple trigons eventually turn into quadragons.

Lastly we must show that no quadragon can remain a quadragon forever. Suppose that Q is a quadragon in a cross-section H. The green sides of Q determine a track-cusp s^{Q}. As we move down, (the branch line containing) s^{Q} is eventually inside a toggle square within a cross-section $K = \partial^- U$. Using Lemma 9.15(5), we observe that the component of $\breve{K} - B^{\mathcal{V}}$ containing s^{Q} has no quadragons. Therefore Q is no longer a quadragon. A similar argument shows that quadragons must eventually become trigons as we move upwards.

This completes the proof that components of $M - (B^{\mathcal{V}} \cup B_{\mathcal{V}})$ are either dynamic shells or pinched tetrahedra.

10.10. **Transience.** Suppose that F is a component of $B_{\mathcal{V}} - B^{\mathcal{V}}$. Choose a point $x \in F$. Let U be a crimped shearing region containing x, and let H be the cross-section of U containing x. Proposition 9.16 implies that there is one ideal vertex v of U in the component of $H - \tau^H$ containing x. Let c be the cusp of M containing v. By Section 10.7, there is a unique dynamic shell C containing c.

Separating $C \cap H$ from x within $H - \tau^H$ is a finite collection of regions R_i of $H - (\tau^H \cup \tau_H)$. As we flow upwards, even when we move from one shearing region to the next, each of these regions evolves according to Definition 4.5. In particular they all eventually collapse. Moreover, by Remark 10.5, no new regions are created between (the image of) x and C. So the image of x eventually flows into an unstable face of C. The same argument applies to components of $B^{\mathcal{V}} - B_{\mathcal{V}}$, flowing downwards.

10.11. **Canonicity and complexity.** In our construction, we make no arbitrary choices. Thus split position is canonical. In particular, if one changes the orientation of the manifold or reverses the direction of the flow then only names will change and not the underlying combinatorics of the dynamic pair.

Now suppose that $\mathcal{V}$ is a finite transverse veering triangulation. Let $|\mathcal{V}|$ denote the number of veering tetrahedra. In building the shearing decomposition (Theorem 5.10), we produce $2|\mathcal{V}|$ half-tetrahedra and perform $2|\mathcal{V}|$ gluings. This requires linear time. In producing the crimped shearing decomposition (Section 5.17), the work is now proportional to the sum of the edge degrees, which is $6|\mathcal{V}|$. This again requires linear time.

To specify the split positions of $B^{\mathcal{V}}$ and $B_{\mathcal{V}}$, it suffices to determine the position of every track-cusp c in each horizontal cross-section H appearing in the Θ–decomposition of every crimped shearing region U. The branch intervals of B^U lie close to the sidings except, possibly, in the lower half of Θ_U. Taking $H = \partial^- U$, and supposing that the siding for c lies in a toggle square, we find that c splits forward in the (space) neighbourhood splitting described in Section 9.5. The path of c is exactly the train route $\beta(c)$ described in Section 9.1. The naive algorithm given there takes time at most quadratic in the degree of the relevant longitudinal edge of U. Since the longitudinal edges partition the sum of the edge degrees, the total complexity of computing the train routes $\beta(c)$ is at most quadratic.

We now bound the number of edges in the dynamic train track $B^{\mathcal{V}} \cap B_{\mathcal{V}}$. Suppose that $(U_i)_{i=1}^m$ is a collection of blue crimped shearing regions with the following properties.

(1) $U = U_1$ has at least one toggle square in $\partial^- U$.
(2) $V = U_m$ has at least one toggle square in $\partial^+ V$.
(3) For $i = 1, 2, \ldots, m-1$, the upper boundary of U_i equals the lower boundary of U_{i+1}.
(4) There are no toggle squares in this shared cross-section.
(5) The length of U, and thus of all of the U_i, is n.

We allow m to be one (and thus $U = V$). We also allow n to be one.

Let H be the lower boundary of $\Theta(U)$. The track τ_H has $2n$ branches (outside of a small neighbourhood of the sidings). Each of these branches is a line segment in H. By Lemma 9.17(3), each branch of τ_H above a toggle square has projection to $\partial^- U$ contained within that toggle square. The remaining branches of τ_H have projections that avoid the toggle squares. Thus no branch of τ_H wraps all the way around H.

Let K be the upper boundary of $\Theta(V)$. By a similar argument, τ^K has $2n$ branches (outside of a small neighbourhood of the sidings). Again, each is a line segment in K. Furthermore, all of these are either below toggle squares or have slope greater than $1/n$. The track τ^H is obtained from τ^K by shearing. After moving from K to the lower boundary of $\Theta(V)$, branches below toggle squares now have large positive slope while all other branches become slightly shallower, and so all branches now have slope greater than $1/(n+1)$. Pushing down through (U_i), we arrive at H. By induction, the branches of τ^H have slope greater than $1/(n+m)$. Thus any branch of τ^H wraps at most $(m+n)/n$ times around H. Thus each branch of τ^H meets each branch of τ_H at most $[(m+n)/n]+1$ times. There are $(2n)^2$ such pairs, for a total of at most $4n(m+2n)$ intersections. This counts all edges of the dynamic train track above Θ_U and below Θ^V. Edges of the dynamic train track either continue or merge in pairs as we descend from H to $\partial^- U$. Thus there are at most an additional $4n(m+2n)$ edges in Θ_U. Likewise there are at most an additional $4n(m+2n)$ edges in Θ^V.

There are now two cases. If $m \geq n$ then the size of the dynamic train track in $\cup_i U_i$ is $O(nm)$; this is proportional to the number of tetrahedra in $\cup_i U_i$. If $m \leq n$ then the size is instead $O(n^2)$; this is bounded above by the square of the number of tetrahedra in $\cup_i U_i$. Summing, we deduce that the size of the dynamic train track is at most quadratic in $|\mathcal{V}|$.

This completes the proof of Theorem 10.1. □

Question 10.12. There is a sequence $(\mathcal{V}_k)_{k=2}^{\infty}$ of veering triangulations with the following properties.

- $\mathcal{V}_k$ has k tetrahedra.
- $\mathcal{V}_{k+1}$ is obtained from $\mathcal{V}_k$ by *horizontal veering Dehn surgery* (along a Möbius band) [16].
- The size of the dynamic train track of $\mathcal{V}_k$ grows quadratically with k.

Thus we may ask if there is some other canonical construction of a dynamic pair which yields a smaller dynamical flow graph. ◇

Appendix A. From equatorial squares to maximal rectangles

App:Rectangles

For our future work, we require an analysis of maximal rectangles in the leaf space for the "flow" associated to a given veering triangulation. We proceed as follows.

Suppose that M is a three-manifold. Suppose that $\mathcal{V}$ is a veering triangulation of M. Let $\mathcal{U}$ be the associated crimped shearing decomposition of M, as defined in Section 5.17.

Def:Cross **Definition A.1.** Suppose that t is a veering tetrahedron of $\mathcal{V}$. Let $E = E(t)$ be its equatorial square. Let e_0, e_1, e_2, and e_3 be the veering edges of E. Recall that $E_c(\mathcal{V})$ is the crimped branched surface. Let n_i be a small regular neighbourhood of e_i taken in $E_c(\mathcal{V})$. Let $s_i = n_i - E$.

Let U and V be the crimped shearing regions above and below s_i respectively. Let H_i be the component of $\partial^- U \cap \partial^+ V$ containing s_i. We define $X = X(t) = E \cup (\cup_i H_i)$ to be the *cross* associated to the tetrahedron t. ◇

As usual, we define $\tau^X = X \cap B^{\mathcal{V}}$, and similarly define τ_X. These are train tracks properly embedded in X. Let $\tau(X) \subset X$ be the graph dual to the union $\tau^X \cup \tau_X$. In a small abuse, we place vertices of $\tau(X)$, if dual to a cusp region, at the associated cusp. We colour an edge e' of $\tau(X)$ green or purple as its dual edge e lies in τ_X or τ^X respectively. A *rectangle* in X is an embedded disk in X whose sides in $\tau(X)$ alternate in colour exactly four times.

Lem:TetRectangle **Lemma A.3.** *There is a unique rectangle $R = R(t)$ in $X = X(t)$ which contains the vertices of t.*

Proof. Fix an edge e of the equatorial square $E = E(t)$. Let c and d be the cusps at the two ends of e. Let Y be the component of $X - e$ not containing E. Suppose that the siding immediately adjacent to c, in Y, lies in τ^Y. Thus the siding immediately adjacent to d, in Y, lies in τ_Y. By Proposition 9.16 there is a (unique) component F of $Y - \tau_Y$ containing c. Similarly there is a component G of $Y - \tau^Y$ containing d. By Lemma 9.15(1) and (2), the regions F and G intersect in a quadragon. We deduce that there is a path in the dual graph (to $\tau^Y \cup \tau_Y$) from c to d that changes colour, from purple to green, exactly once. See Figure A.2.

Suppose that the siding immediately adjacent to c, in Y, instead lies in τ_Y. Then a similar argument finds a path in the dual graph from c to d that changes colour, from green to purple, exactly once.

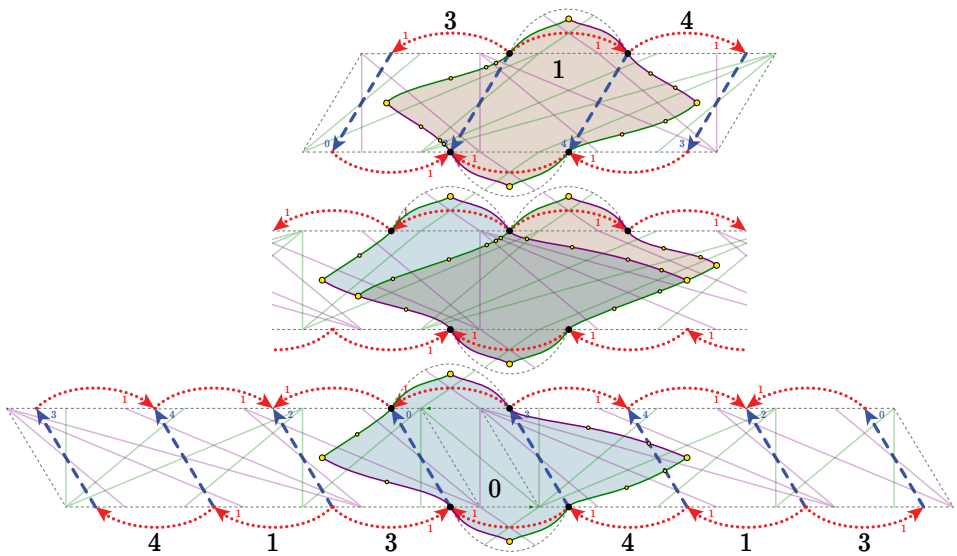

FIGURE A.2. The first row shows the cross for the equatorial square for tetrahedron 1 in `fLLQccecddehqrwjj_20102`. The third row shows the cross for the equatorial square for tetrahedron 0. In both cases the maximal rectangle is shaded in grey. The second row shows the T-shape for the unique face shared by tetrahedra 1 and 0. The face rectangle is shaded in dark grey. The vertices and edges of the dual graph are shown only on the boundary of the rectangles. The cusps are shown with black dots while other regions are indicated with yellow dots. Corners of the rectangles are drawn with larger yellow dots.

Fig:Crosses

Doing the above for all four edges of E gives the boundary of the desired rectangle $R = R(t)$. Since ∂R contains one cusp in each of its four (monochromatic) sides, R is maximal and thus unique. $\square$

Note that $R(t)$ receives a cellulation from its intersection with τ^X and τ_X. We use $R^{(1)}(t)$ to denote the edges of $R(t)$ belonging to τ^X. Similarly, $R_{(1)}(t)$ denotes the edges of $R(t)$ belonging to τ_X. We now turn to constructing rectangles for the faces of $\mathcal{V}$.

Def:TShape **Definition A.4.** Suppose that f is a veering face of $\mathcal{V}$. Let e_0, e_1, and e_2 be its veering edges. Two of these, say e_1 and e_2 are the same colour. Let c_i be the vertex of f opposite e_i. Let W' be the shearing region (in the shearing decomposition), containing f. Let W be the corresponding crimped shearing region. The edges e_1 and e_2 are helical in ∂U; also there is a longitudinal crimped edge e_0' in ∂U that cobounds a crimped bigon B with e_0. Let n_0 be a small regular neighbourhood of e_0 taken in $E_c(\mathcal{V})$. Let $s_0 = n_0 - B$.

Let U and V be the crimped shearing regions above and below s_0 respectively. Let H_0 be the component of $\partial^- U \cap \partial^+ V$ containing s_0. We take H to be the central cross-section of $\Theta(W)$. We define $T = T(f) = H \cup H_0$ to be the *T-shape* associated to f. ◇

The proof of the following is similar to that of Lemma A.3, replacing Lemma 9.15 by Lemma 9.17.

Lem:FaceRectangle **Lemma A.5.** *There is a unique rectangle $R = R(f)$ in $T = T(f)$ which contains the vertices of f.* □

Again, $R(f)$ receives a cellulation from the tracks τ^T and τ_T.

Prop:Flow **Proposition A.6.** *Suppose that f is an upper face of the tetrahedra t in $\mathcal{V}$. Let $T = T(f)$ and $X = X(t)$. The natural flow from $R(f) \subset T$ to $R(t) \subset X$ takes*

- *distinct cusps to distinct cusps;*
- *vertices to vertices;*
- *edges of $R^{(1)}(f)$ to edges of $R^{(1)}(t)$;*
- *edges of $R_{(1)}(f)$ to vertices, or to edges of $R_{(1)}(t)$; and*
- *faces of $R(f)$ to either edges of $R^{(1)}(f)$, or to faces of $R(t)$.*

There is a similar statement when f is a lower face of t. □

References

[1] Ian Agol. Ideal triangulations of pseudo-Anosov mapping tori. In *Topology and geometry in dimension three*, volume 560 of *Contemp. Math.*, pages 1–17. Amer. Math. Soc., Providence, RI, 2011, `arXiv:1008.1606`. [1, 5]

[2] Ian Agol and Chi Cheuk Tsang. Dynamics of veering triangulations: infinitesimal components of their flow graphs and applications, 2022, `arXiv:2201.02706`. [3, 26]

[3] Benjamin A. Burton, Ryan Budney, William Pettersson, et al. Regina: Software for low-dimensional topology, 1999–2021. [26]

[4] Danny Calegari. Bounded cochains on 3-manifolds, 2001. [3]

[5] Danny Calegari. *Foliations and the geometry of 3-manifolds*. Oxford Mathematical Monographs. Oxford University Press, Oxford, 2007. [3, 6, 8]

[6] McA. Gordon Cameron. The theory of normal surfaces. Based on lecture notes; typeset by Autumn Kent. [7]

[7] Baris Coskunuzer. Uniform 1-cochains and genuine laminations. *Topology*, 45(4):751–784, 2006. [3]

[8] Marc Culler, Nathan Dunfield, and Jeffrey R. Weeks. SnapPy, a computer program for studying the geometry and topology of three-manifolds. [21]

[9] Sérgio R. Fenley. Foliations with good geometry. *J. Amer. Math. Soc.*, 12(3):619–676, 1999. [3]

[10] Steven Frankel, Saul Schleimer, and Henry Segerman. From veering triangulations to link spaces and back again. Preprint. [3, 7]

[11] Andreas Giannopolous, Saul Schleimer, and Henry Segerman. A census of veering structures. [19, 21, 26]

[12] Craig D. Hodgson, J. Hyam Rubinstein, Henry Segerman, and Stephan Tillmann. Veering triangulations admit strict angle structures. *Geom. Topol.*, 15(4):2073–2089, 2011, `arXiv:1011.3695`. [1, 4, 5, 26]

[13] Marc Lackenby. Taut ideal triangulations of 3-manifolds. *Geom. Topol.*, 4:369–395, 2000, `arXiv:math/0003132`. [4, 7]

[14] Lee Mosher. Laminations and flows transverse to finite depth foliations. Preprint, 1996. [1, 3, 8, 9, 10, 12]

[15] R. C. Penner and J. L. Harer. *Combinatorics of train tracks*, volume 125 of *Annals of Mathematics Studies*. Princeton University Press, Princeton, NJ, 1992. [5]

[16] Saul Schleimer and Henry Segerman. Veering Dehn surgery. In preparation. [19, 60]

[17] Saul Schleimer and Henry Segerman. Essential loops in taut ideal triangulations. *Algebr. Geom. Topol.*, 20(1):487–501, 2020, `arXiv:1902.03206`. [3]

[18] Saul Schleimer and Henry Segerman. From loom spaces to veering triangulations, 2021, `arXiv:2108.10264`. [3]

[19] William P. Thurston. Geometry and topology of three-manifolds. Lecture notes, 1978. [3, 5]

[20] Chi Cheuk Tsang. Constructing Birkhoff sections for pseudo-Anosov flows with controlled complexity, 2022, `2206.09586`. [2]

[21] Chi Cheuk Tsang. Veering branched surfaces, surgeries, and geodesic flows, 2022, `2203.02874`. [19]